ELSEVIER

FEMS Microbiology Reviews 22 (1999) 567–598

FEMS MICROBIOLOGY REVIEWS

Elucidation of novel biosynthetic pathways and metabolite flux patterns by retrobiosynthetic NMR analysis

Adelbert Bacher [a,*], Christoph Rieder [a], Dietmar Eichinger [a], Duilio Arigoni [b], Georg Fuchs [c], Wolfgang Eisenreich [a]

[a] *Lehrstuhl für Organische Chemie und Biochemie, Technische Universität München, Lichtenbergstr. 4, D-85747 Garching, Germany*
[b] *Laboratorium für Organische Chemie, ETH Zürich, Universitätsstr. 16, CH-8092 Zürich, Switzerland*
[c] *Institut für Biologie II, Albert-Ludwigs-Universität Freiburg, Schänzlestr. 1, D-79104 Freiburg, Germany*

Received 17 July 1998; received in revised form 12 October 1998; accepted 13 October 1998

Abstract

The labelling patterns of metabolites from experiments with stable isotope-labelled precursors can be determined by NMR spectroscopy. Complex isotopomer mixtures are found when general metabolites such as glucose are used as stable isotope-labelled precursors which are diverted to all branches of intermediary metabolism. The complex results can be interpreted by a pattern recognition approach based on comparison between the labelling patterns of secondary metabolites and primary metabolites such as amino acids and ribonucleosides. The isotope labelling patterns of intermediates in central metabolic pools such as carbohydrate phosphates, dicarboxylic acids, and acetyl CoA can be obtained by biosynthetic retroanalysis. Biosynthetic pathways as well as metabolite flux patterns can be determined from these data. The method is illustrated using the classical mevalonate pathway and the more recently discovered deoxyxylulose pathway of terpenoid biosynthesis as examples. Applications of the retrobiosynthetic method of the biosynthesis of molybdopterin and of riboflavin are also discussed. Stable isotope experiments monitored by NMR spectroscopy have also been shown to be a powerful tool for the elucidation of metabolic flux in microorganisms with unusual lifestyles and in fermentation processes.

Keywords: NMR spectroscopy; Retrobiosynthetic analysis; CO_2 fixation; Biosynthesis of terpenoids; Biosynthesis of molybdopterin; Metabolic flux

Contents

* Corresponding author. Tel.: +49 (89) 289-13360; Fax: +49 (89) 289-13363; E-mail: bacher@bionmr.org.chemie.tu-muenchen.de

0168-6445/99/$19.00
PII: S0168-6445(98)00034-5

1. Introduction

The use of isotopically labelled organic compounds as tracers for the elucidation of metabolic pathways in organisms, tissues and cells is a time-honoured concept. The earliest tracer studies were conducted with deuterium in the 1930s [1]. For an early review of the applications of isotopes in biochemistry in which stable isotopes play a dominant role see Kamen [2]. A milestone for the application of carbon isotopes for more than a decade was the book entitled *Isotopic Carbon* compiled by Calvin and other early pioneers in this field [3]. Subsequently, the era of tracer studies with radiolabelled compounds was ushered in when compounds labelled with ^{14}C, ^{32}P, ^{35}S and later with ^{3}H became commercially available in the 1950s and 1960s. The radiolabels had the enormous advantage of high detection sensitivity. Minute amounts of metabolites were sufficient for analysis, and the introduction of liquid scintillation counters with energy discrimination afforded convenient detection [4,5].

Whereas it had become easy to detect the radiolabels with excellent sensitivity, it was not always easy to make sure that the detected radioactivity actually formed part of the metabolite under study as opposed to a contamination with another radiolabelled compound. Studies with radioactively labelled biochemicals were especially fruitful in combination with the various methods of chromatography and electrophoresis. Actually the combination of both methods caused the enormous progress of biochemistry in the second part of this century.

However, even under stringent conditions of purification and analysis, the position of the radioactive label in the metabolite under study remained unknown. Positional information could be obtained by chemical degradation procedures affording pure samples of discrete molecular fragments. Even with relatively simple compounds, the dissection of metabolites to the level of individual carbon and/or hydrogen atoms was a very laborious process requiring sophisticated chemical methodology [4]. With structurally complex metabolites, rigorous dissection became simply impossible. Despite these caveats, the merit of the radiolabel methods for the elucidation of metabolic pathways was enormous. However, it should also be noted that the literature shows numerous incorrect or partly incorrect conclusions based on these methods, especially in cases where relatively low incorporation levels were used to construct a biosynthetic relationship between a specific precursor and a downstream metabolite.

Tracer studies with stable isotopes became routinely feasible in the wake of mass spectrometry and NMR technology. The specific features of these detection methods can be summarised as follows. (i) Very little sample material is required for mass spectrometry, whereas relatively large samples in the μmol range are required for NMR spectroscopy, even with modern instrumentation. (ii) The specific position of the heavy isotope label in the metabolite under study can be determined with high accuracy by NMR; as a prerequisite, all NMR signals of the metabolites must be unequivocally assigned. Assignment of the label to certain molecular fragments is also possible by mass spectrometry, but the unequivocal assignment of the label to a single atom position is not easily achieved. (iii) NMR spectroscopy can unequivocally detect the presence of the isotope even in cases of low incorporation rates; ^{13}C label can be reliably detected when the ^{13}C abundance at the labelled atom position is at least 1.5 times above the natural abundance of ^{13}C (1.1%). The detection of isotopomers which have acquired several contiguous ^{13}C atoms from a multiply labelled precursor can be detected by NMR at even higher sensitivity. On the other hand, the sensitivity of mass spectrometry in cases with poor incorporation rates is rather limited. (iv) Multiple labelling can be detected by both analytical methods.

The simplest hypothesis for the interpretation of a

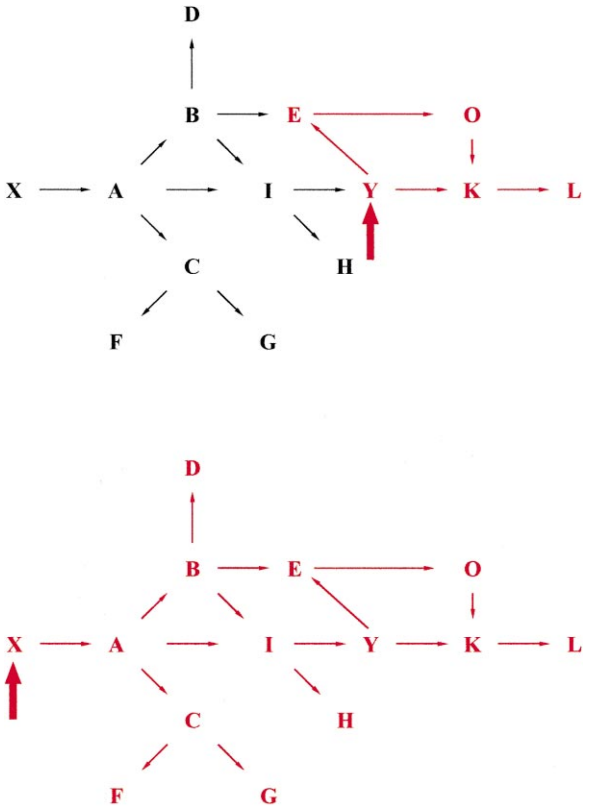

Fig. 1. Use of a specialised metabolite (e.g. Compound y; top) and of general metabolic precursors (e.g. Compound x; bottom) for biosynthetic tracer experiments.

stable isotope incorporation experiment assumes that the label from one specific position in the precursor molecule is specifically transferred to one specific position in the target metabolite pathway. Based on this hypothesis, the traditional approach for isotope incorporation studies usually implied an educated guess of a plausible precursor based on the chemical structure of the terminal metabolite under study. The candidate compound was then proffered in labelled (radiolabelled isotope or stable isotope) form to an organism or cell culture. The metabolite under study was then isolated, and its isotope content was determined. Incorporation of label was accepted as evidence that the proffered compound had acted as a specific metabolic precursor for the metabolite under study. This deduction implies that there is one and only one metabolic pathway from the precursor to the final metabolite.

In reality, many precursors will be able to serve as substrate for a variety of metabolic pathways. Consequently, label will be distributed to various metabolic pools with different efficacy, and at least a fraction of the isotopic label may reach the target metabolite after more or less extensive reshuffling in the general metabolism. From these intermediary metabolites, a variety of different isotopomers of the metabolite under study can be generated. In other words, label from one specific position in the precursor can end up in different positions of the target molecule. Consequently, the isotopomer mixtures can be complex and the ultimate arrival of the isotope in the metabolite under study does not answer the question whether the isotope was diverted via a relatively direct way or via a complex network of interconnected metabolic pathways (Fig. 1).

In contrast to the use of specific precursors with close structural relationships with the terminal metabolite, the retrobiosynthetic approach preferen-

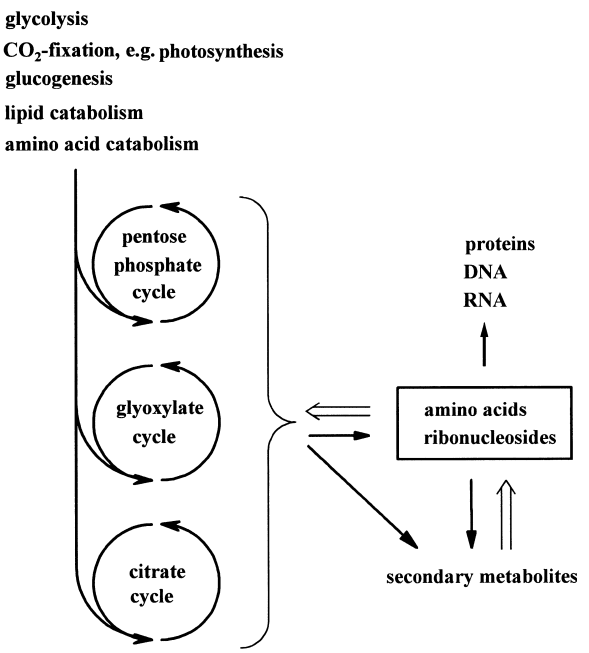

Fig. 2. Biosynthesis of secondary metabolites from central metabolic intermediates and/or primary metabolites. Reconstruction of central labelling patterns and biosynthetic pathways by pattern recognition are indicated by the symbol ⇒.

tially uses general metabolites, e.g. glucose, ribose, glycerol, pyruvate or acetate. Each of these compounds can be converted to a wide variety of different metabolites. This diversion of label to a variety of metabolic products can be assessed by hydrolysis of biomass followed by isolation of amino acids and ribonucleotides. The isotopomer pattern can then be determined quantitatively for each compound by NMR spectrometry.

All biosynthetic pathways utilise starting materials derived from central metabolic pathways (e.g. glycolysis, pentose phosphate cycle, citrate cycle) (Fig. 2). These central intermediates can be recruited for the biosynthesis of complex metabolites via the products of primary metabolites (amino acids, nucleic acid components) or via more direct routes. The labelling patterns of the central intermediate pool (e.g. acetyl CoA, trioses, dicarboxylic acids) are ordinarily elusive, because the central intermediates represent only a small fraction of biomass and can therefore not be isolated in sufficient amounts for direct analysis. However, labelling patterns of the elusive central metabolites can be reconstructed with high fidelity from the labelling patterns of amino acids and ribonucleotides.

In analogy to the retrosynthetic concept of synthetic organic chemistry, we use the symbol ⇒ to indicate the biosynthetic connection between the labelling pattern of the terminal metabolite and its biosynthetic precursor. It should be noted that the retrobiosynthetic relationships shown are not universal but must be determined explicitly for the organism under study. Specific metabolic flux patterns for the eubacterium *Chloroflexus aurantiacus* [6] and the plant *Beta vulgaris* (Werner, Eisenreich and Bacher, unpublished) are shown in Figs. 3 and 4.

As an example of the retrobiosynthetic analysis, the labelling pattern of the ribose phosphate pool is faithfully reflected in the glycoside moieties of ribonucleotides which can be obtained by hydrolysis of cellular RNA; if several ribonucleotides are analysed, the accuracy of the analysis can be checked statistically. Labelling patterns of other central metabolites can be reconstructed from NMR analysis of amino acids which can be isolated after hydrolysis of cell mass. For example, the labelling pattern of the acetyl CoA pool can be determined from leucine, the labelling pattern of oxaloacetate is reflected in cellular aspartate, and the labelling pattern of ketoglutarate is easily gleaned from glutamate.

The use of multiply ^{13}C-labelled or uniformly ^{13}C-labelled precursors (e.g. [U-$^{13}C_6$]glucose, [U-$^{13}C_2$]-acetate, [U-$^{13}C_5$]ribose) can be particularly informative. They must be proffered together with a large excess of unlabelled precursor. The universally labelled precursors can be fragmented by catabolic processes, and the resulting metabolites can be reassembled under formation of secondary metabolites. If the labelled precursor is proffered together with a large amount of unlabelled material, the resulting secondary metabolites will be mosaics assembled from labelled as well as unlabelled modules. The site of the building blocks is easily gleaned from this mosaic pattern (for details see below). These feeding experiments usually afford isotopomers with several ^{13}C atoms which have been jointly transferred from a single precursor molecule. Frequently, the isolated metabolites are complex isotopomer mixtures since isotope from the general precursors can usually be diverted to a certain metabolite via

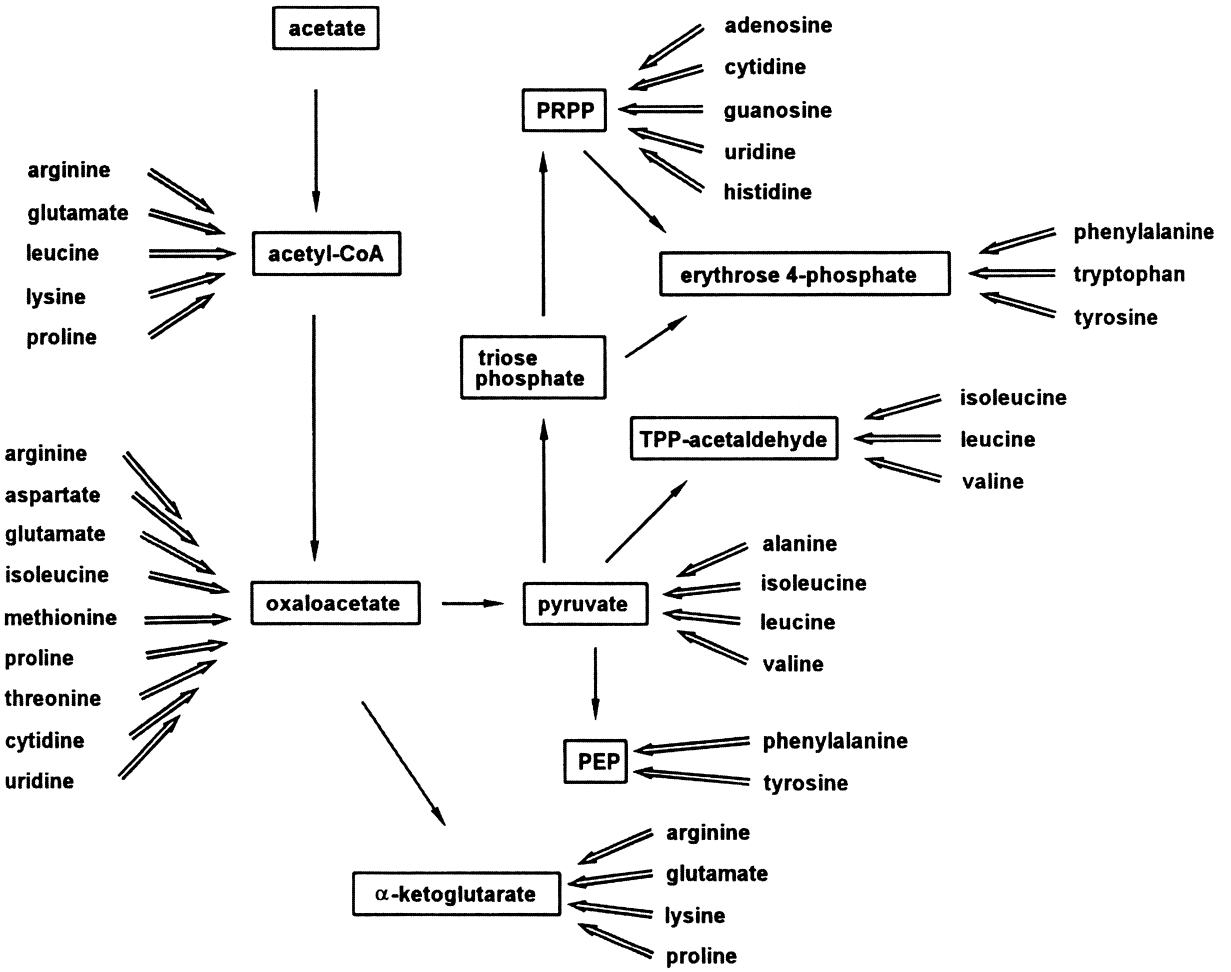

Fig. 3. Retrobiosynthetic analysis of acetate utilisation in *Chloroflexus aurantiacus* [6].

more than one route. Moreover, the labelled precursor can be recycled extensively by cyclic metabolic processes, which can result in positional redistribution of isotope.

For these reasons, the ^{13}C NMR signals of metabolites biosynthesised from multiply ^{13}C-labelled precursors can be quite complex. As an example, the ^{13}C NMR signature of carbon atom 3 of gallic acid (**1**) obtained biosynthetically from a mixture of [U-$^{13}C_6$]glucose and unlabelled glucose consists of 25 lines (Fig. 5) [7]. They can be attributed unequivocally to five different isotopomers, and the isotopomer composition of the sample could be determined accurately. The interpretation of such complex spectra is sometimes laborious. Spectral simulation and deconvolution techniques, as well as advanced one-dimensional and two-dimensional NMR experiments, such as ^{13}C TOCSY and INADEQUATE, are important for detailed analysis.

The joint transfer of several ^{13}C atoms en bloc from a multiply ^{13}C-labelled precursor documents that the bonds between the respective atoms have remained intact during the passage of the fragment through intermediary metabolism. The concept is therefore addressed metaphorically as 'bond labelling'. Determining the number of carbon atoms which can be transferred en bloc affords rigorous constraints for the intermediary pathway through which the metabolic fragment has been processed.

Since terminal metabolites are ultimately derived

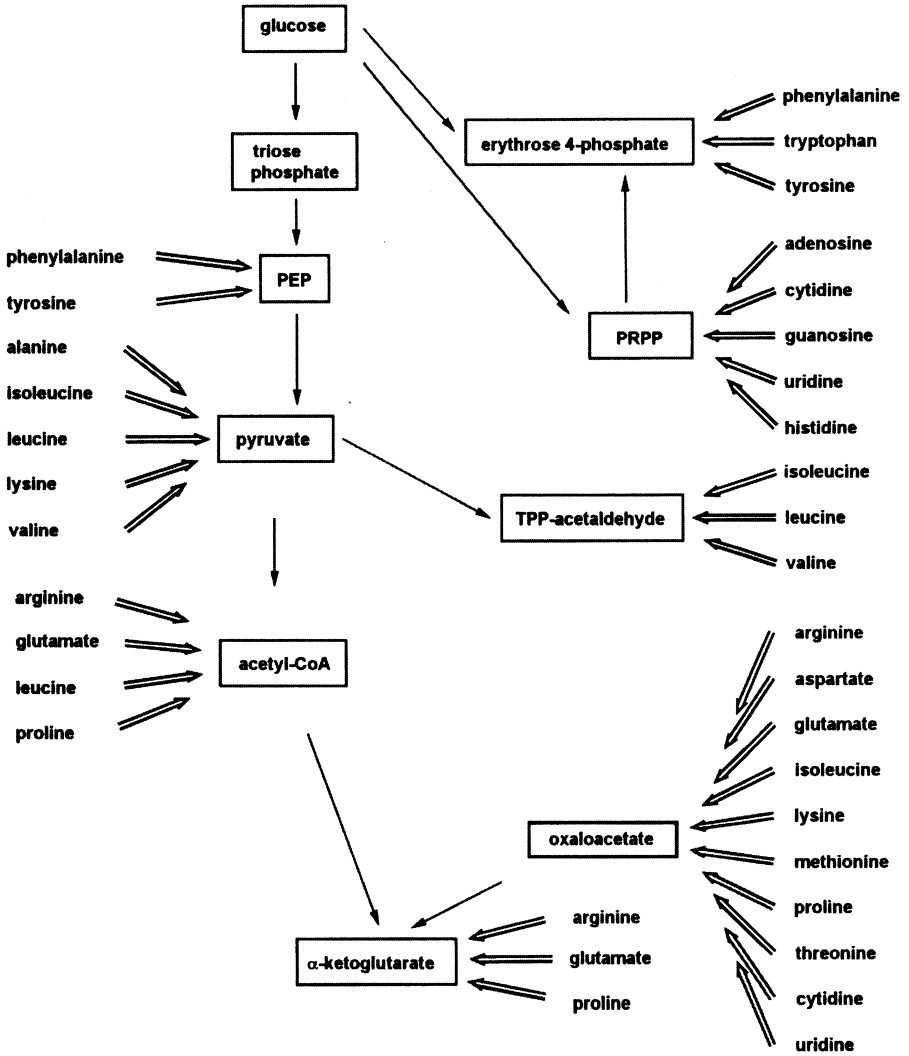

Fig. 4. Retrobiosynthetic analysis of glucose utilisation in cultures of higher plant cells as determined with *Taxus chinensis*, *Rubia tinctorum*, *Rauwolfia serpentina* and *Beta vulgaris*.

from the central metabolic pools of intermediary metabolism such as carboxylic acids (e.g. acetate), dicarboxylic acids (e.g. succinate), or carbohydrates (e.g. triose phosphate, tetrose phosphate, pentose phosphate), their labelling patterns must reflect the labelling patterns of the primary metabolites from which they have been assembled in the biosynthetic process. It is therefore possible to determine the early precursors of terminal metabolites by a pattern recognition approach based on comparison between the labelling patterns of different cellular metabolites. In other words, the isotopomer pattern of a terminal metabolite is treated as a puzzle, and the intermediates of primary metabolism are the pieces which must be assembled properly. Labelling strategies conducive to multiple labelling of intermediary metabolites (with ^{13}C, ^{2}H, ^{15}N) are particularly appropriate for this approach because the spin systems of the resulting, multiply labelled metabolites can be elegantly assessed by NMR correlation spectroscopy in one or more dimensions.

An important caveat must be considered for the

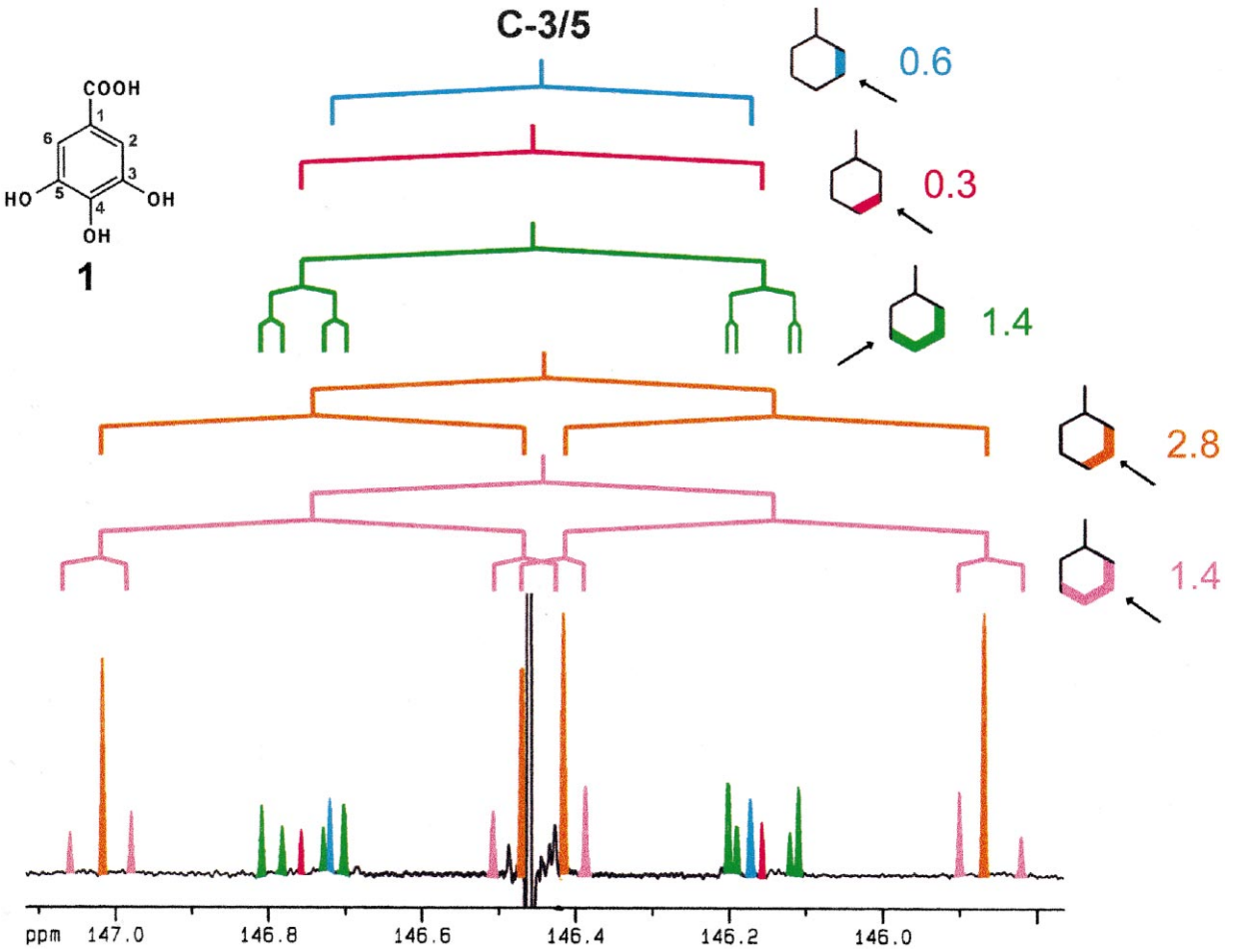

Fig. 5. ^{1}H decoupled ^{13}C NMR signals of the homotopic carbon atoms C3 and C5 of gallic acid from *Phycomyces blakesleeanus* after incorporation of [U-$^{13}C_6$]glucose diluted with unlabelled glucose (1:25, w/w). Black arrows indicate the observed carbon atom in each respective isotopomer. Multiple labelling of the different isotopomers is indicated by coloured bars connecting the groups of carbon atoms in each respective isotopomer shown schematically on the right. Isotopomers and their corresponding signals are shown in identical colours. The numbers indicate absolute isotopomer contributions from [U-$^{13}C_6$]glucose in mol %.

correct application of the retrobiosynthetic concept. Whereas the pathways for some metabolites such as aromatic amino acids are unique, other metabolites such as lysine can be obtained via alternative pathways in different organisms. Moreover, a given metabolite, e.g., serine, may be obtained via different, parallel pathways in the same organism. This type of information is important for the correct reconstruction of central metabolite pathways from terminal metabolites, i.e. amino acids and nucleosides. The required information is frequently not available at the outset of retrobiosynthetic analysis but can be obtained from the very labelling data of the amino acids and nucleosides. Superficially, this may appear to be a circular argument. However, if labelling data for all ribonucleosides and amino acids are obtained, the experimental system is sufficiently overdetermined to allow the simultaneous determination of alternative pathways and partitioning factors for multiple pathways as well as labelling patterns of central intermediates. There is insufficient space to elaborate on this claim in the present article, and the reader is directed to specific experimental studies for documentation [7–10].

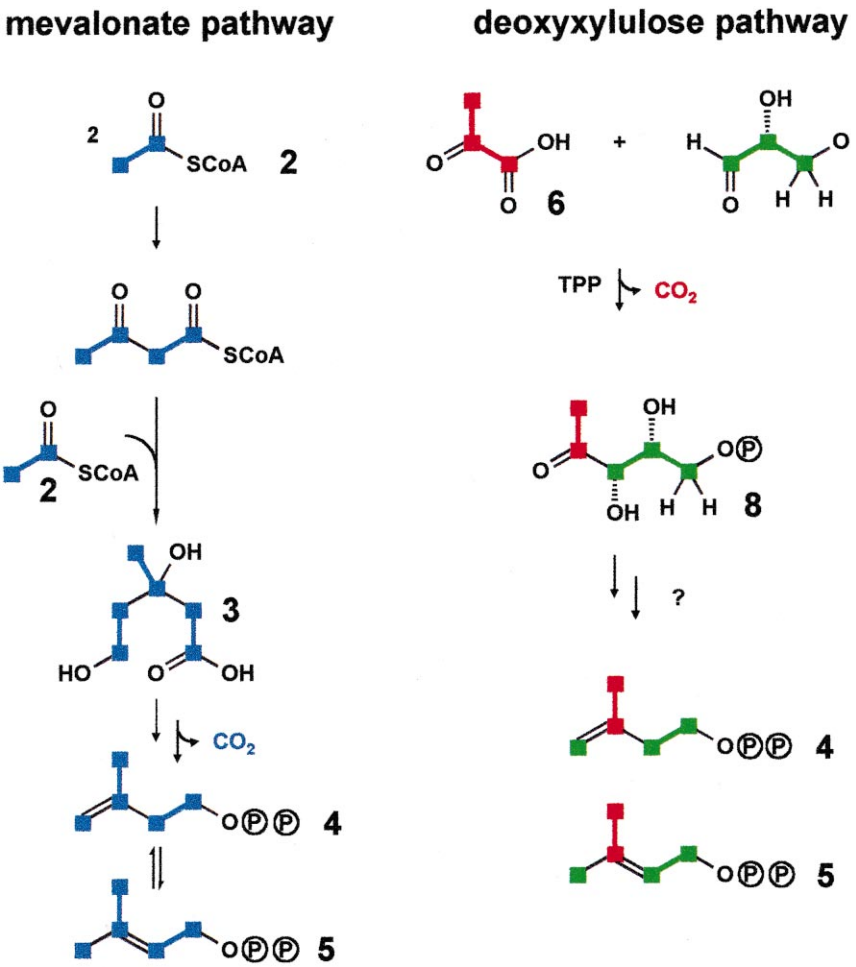

Fig. 6. Diversion of carbon atoms from precursors to isoprenoid monomers by the mevalonate pathway (precursor, acetyl CoA) and the deoxyxylulose pathway (precursors pyruvate and glyceraldehyde 3-phosphate) [8,10,16–19,45,106,114,117,118]. The deoxyxylulose pathway involves a rearrangement of 1-deoxyxylulose 5-phosphate which interrupts the contiguity of the carbon atoms derived from the triose phosphate precursor.

Finally, the labelling patterns of central metabolite pools reconstructed as described above can be used to predict the labelling which should result when a terminal metabolite is generated via any one of different hypothetical pathways. The patterns predicted for different pathways can then be compared with the experimental labelling pattern of the metabolite under study. Incorrect hypotheses afford labelling predictions which are at odds with the experimental results and can therefore be ruled out with a high

→

Fig. 7. Biosynthesis of verrucosan-2β-ol (**9**) in *Chloroflexus aurantiacus*. A: IUPAC conventions. B: Highly enriched carbon atoms acquired from [1-^{13}C]acetate and [2-^{13}C]acetate are shown in green and blue, respectively. C: Pairs of incorporated ^{13}C atoms from [1,2-$^{13}C_2$]acetate are connected by red bars. D: Dissection of isoprenoid monomers on the basis of the cyclisation mechanism proposed in Fig. 8; carbon atoms contributed by individual monomers are boxed. E–G: Parts of ^{13}C NMR spectra of verrucosan-2β-ol; $^{13}C^{13}C$ coupling patterns as identified by INADEQUATE experiments are indicated at the top of the spectra. E: Natural ^{13}C abundance. F: From [2-^{13}C]acetate. G: From [1,2-$^{13}C_2$]acetate. H: Part of a two-dimensional INADEQUATE spectrum of verrucosan-2β-ol from a growth experiment with [1,2-$^{13}C_2$]acetate. The $^{13}C^{13}C$ coherence observed between C-1 and C-2 lies outside the spectral range shown.

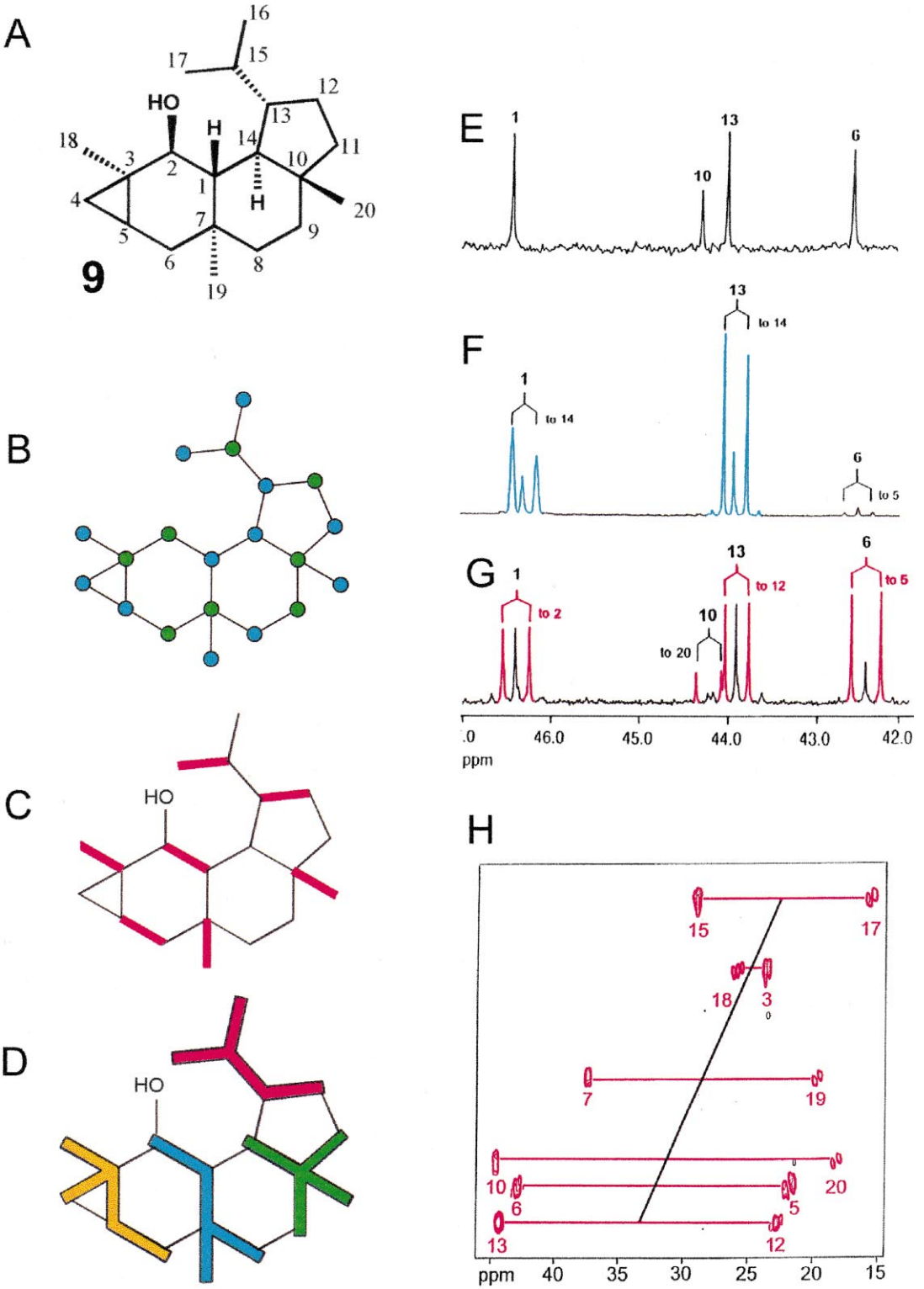
A
16
17
15
12
HO
13
H
14
18
3
2
11
10
1
4
H
20
7
5
9
6
8
19
9
B
C
HO
D
HO
E
1
13
10
6
F
13
to 14
1
to 14
6
to 5
G
1
to 2
13
to 12
6
to 5
10
to 20
.0
46.0
45.0
44.0
43.0
42.0
ppm
H
15
17
18
3
7
19
10
20
6
5
13
12
ppm
40
35
30
25
20
15

degree of certainty. The procedure will be illustrated in Section 2.

It should be noted that the retrobiosynthetic concept can operate with any isotope-labelled precursors, irrespective of the specific structure, provided that the precursor does not lead to a uniform distribution of the isotope label in the organism studied. Incidentally, such a state of total isotope randomisation would represent a maximum of the isotopomer entropy term. It should also be noted that the method works most reliably when several experiments are performed with different precursors (i.e. precursors with different structure or with different labelling pattern). The deconvolution of the labelling patterns by the pattern recognition method can then be cross-checked, thus increasing the reliability.

On the other hand, it is sometimes important to generate a specific isotopomer in one of the central pools in order to answer a specific question. An example where it was important to generate a sufficient level of [U-$^{13}C_5$]isotopomers in the pentose pool will be given in the description of molybdopterin biosynthesis.

2. Biosynthesis of isoprenoids

Dimethylallyl pyrophosphate (**5**, DMAPP) and isopentenyl pyrophosphate (**4**, IPP) have been shown to act as the universal precursors for the biosynthesis of terpenoids. The formation of IPP and DMAPP from three acetyl CoA moieties (**2**) via mevalonate (**3**) has been elucidated by classical studies of Bloch, Lynen, Cornforth and their coworkers using yeast and animal cells (Fig. 6) (for review see [11–14]). For several decades, it was assumed that mevalonate is the universal precursor of isoprenoids, even in cases where the experimental results were not easily harmonised with the prevailing dogma.

Relatively recent studies by Rohmer, Sahm, Arigoni, and their coworkers showed the existence of an alternative pathway (for review see [15]). Specifically, the incorporation of various ^{13}C-labelled glucose isotopomers into hopanoids by some anaerobic eubacteria studied by Rohmer and his coauthors were shown to be inconsistent with the expectations based on the mevalonate pathway [16,17]. Independent experiments of the research group of Arigoni showed that quinoid coenzymes in *Escherichia coli*, ginkgolides in seedlings of *Ginkgo biloba*, and ferruginol in cell cultures of *Salvia milthiorrhiza* were not of mevalonoid origin ([18,19]; Cartayrade and Arigoni, quoted in [19]).

The data were best explained by the formation of IPP and DMAPP via condensation of a three-carbon fragment with a two-carbon fragment followed by a skeletal rearrangement. Obviously, the incorporation of a three carbon fragment from a single precursor molecule is not compatible with the mevalonate pathway, since mevalonate is obtained exclusively from a two-carbon moiety, i.e. acetate.

Subsequent studies showed that glyceraldehyde 3-phosphate (**7**) served as the specific three-carbon compound, and that the two-carbon fragment was derived from pyruvate (**6**) by the loss of the carboxylic group (Fig. 6) [17–19]. Arigoni and his coworkers could then show that the condensation product of the two fragments was 1-deoxy-D-xylulose (or its 5-phosphate, **8**) serving as the committed precursor ([18,19]; Arigoni and Cartayrade as quoted in [19]); the same compound had been shown earlier to serve as precursor for the biosynthetic pathways of thiamin ([20–23]; for review see [24]) and pyridoxal phosphate [22,25].

Enzymes catalysing the formation of 1-deoxy-D-xylulose 5-phosphate from glyceraldehyde 3-phosphate and pyruvate have been obtained recently from *E. coli* and from plants [26–29]. The amino acid sequence of these enzymes is similar to that of transketolases. However, the formation of 1-deoxy-D-xylulose from unphosphorylated glyceraldehyde and pyruvate had also been shown earlier to be catalysed non-specifically by pyruvate dehydrogenase from *E. coli* [30].

The 1-deoxy-D-xylulose pathway has been shown to be responsible for the biosynthesis of terpenoids in a number of eubacteria whereas methanogenic archaea generate terpenoids via the mevalonoid pathway as shown by genomic as well as biochemical evidence (for review see [15]). However, the occurrence of the two pathways in different microbial phyla requires further study.

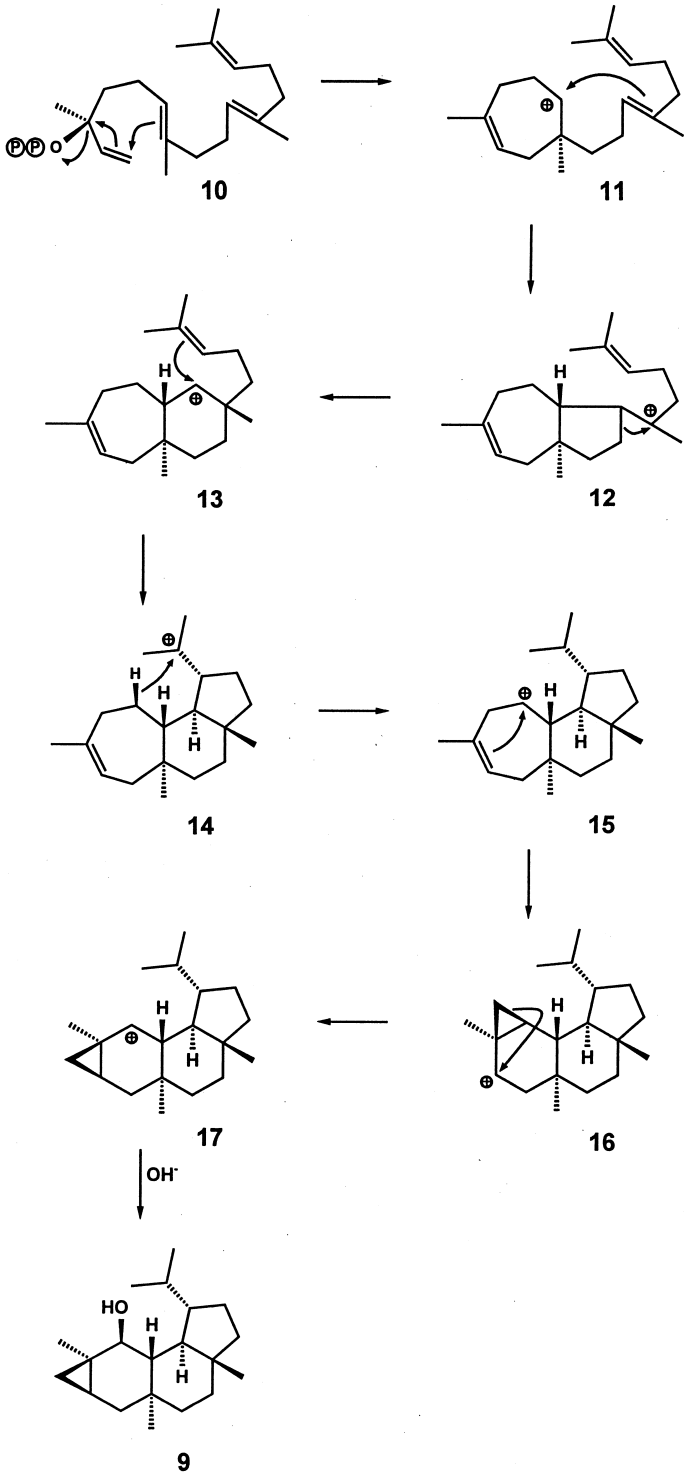

Fig. 8. Hypothetical mechanism for the formation of verrucosan-2β-ol in *Chloroflexus aurantiacus*.

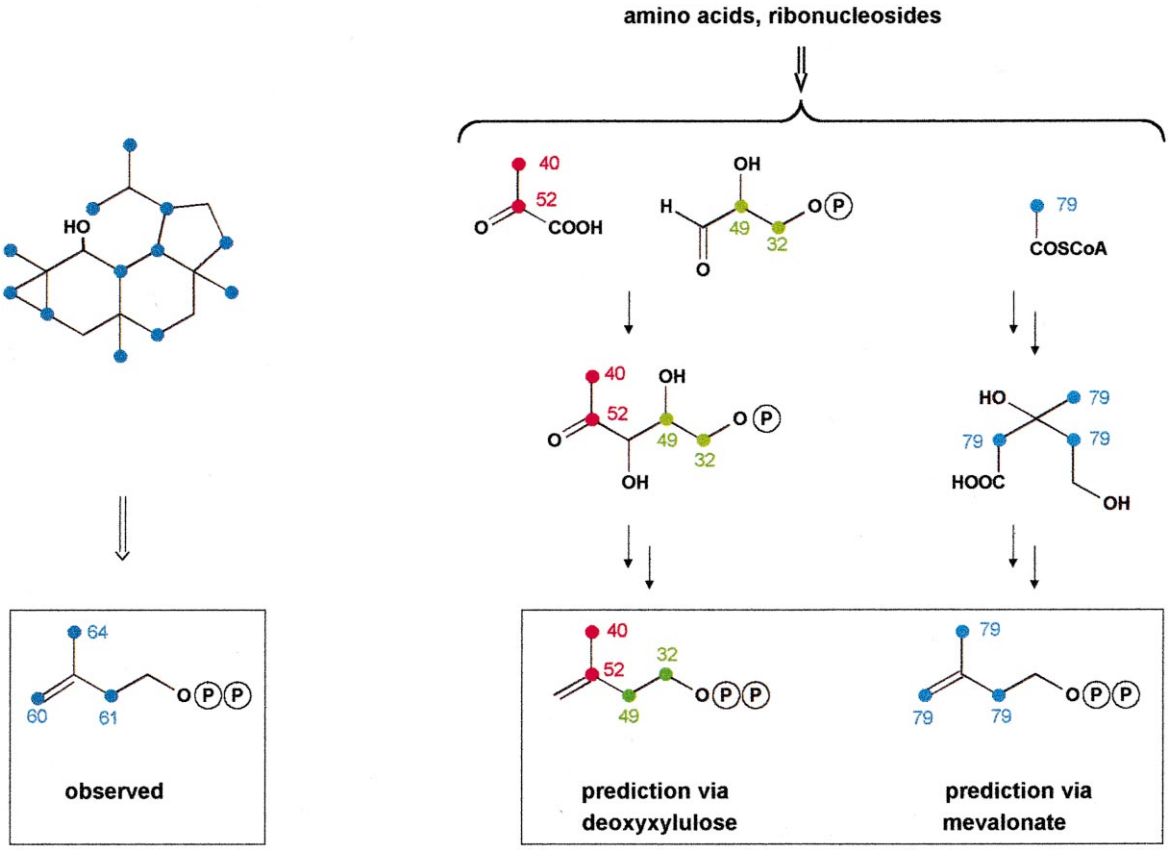

Fig. 9. Retrobiosynthetic analysis of verrucosan-2β-ol biosynthesis. Left: Observed labelling pattern after feeding with [2-^{13}C]acetate. Right: Labelling patterns of IPP predicted via the deoxyxylulose pathway and via the mevalonate pathway.

3. Biosynthesis of the diterpene verrucosanol in the anaerobic eubacterium *Chloroflexus aurantiacus*

C. aurantiacus is a facultatively anaerobic, photosynthetic eubacterium. The microorganism represents the most proximal known branch of a phototropic eubacterium [31–33]. The central metabolism of the microorganism is switched from autotrophism to a heterotrophic mode when acetate is present in the culture medium. However, the autotrophic growth pattern persists when acetate is continuously added to the culture fluid at a low rate. Thus, feeding of ^{13}C-labelled acetate can then be used to diagnose the metabolic pathways of the microorganism under autotrophic as well as under heterotrophic growth conditions.

Cells grown with different isotopomers of acetate afforded amino acid labelling patterns which could be used to reconstruct the labelling pattern of central metabolites (for details see below) (Fig. 3) [6,34]. Verrucosan-2β-ol (**9**, Fig. 7A), one of only four known bacterial diterpenes [35], has been isolated for the first time from cells of *C. aurantiacus* by Hefter et al. [36]. Some of the ^{13}C NMR signals of a sample of **9** isolated from cells supplemented with [U-$^{13}C_2$]acetate are shown in Fig. 7G. The ^{13}C signals appear as multiplets consisting of a central line flanked symmetrically by $^{13}C^{13}C$ coupling satellites. The ^{13}C NMR spectrum of a verrucosan-2β-ol sample obtained from cells grown without ^{13}C-labelled acetate is shown for comparison in Fig. 7E. In this sample, all ^{13}C signals appear as singlets originating from the natural abundance ^{13}C contribution of 1.1%. The coupling patterns in the samples from

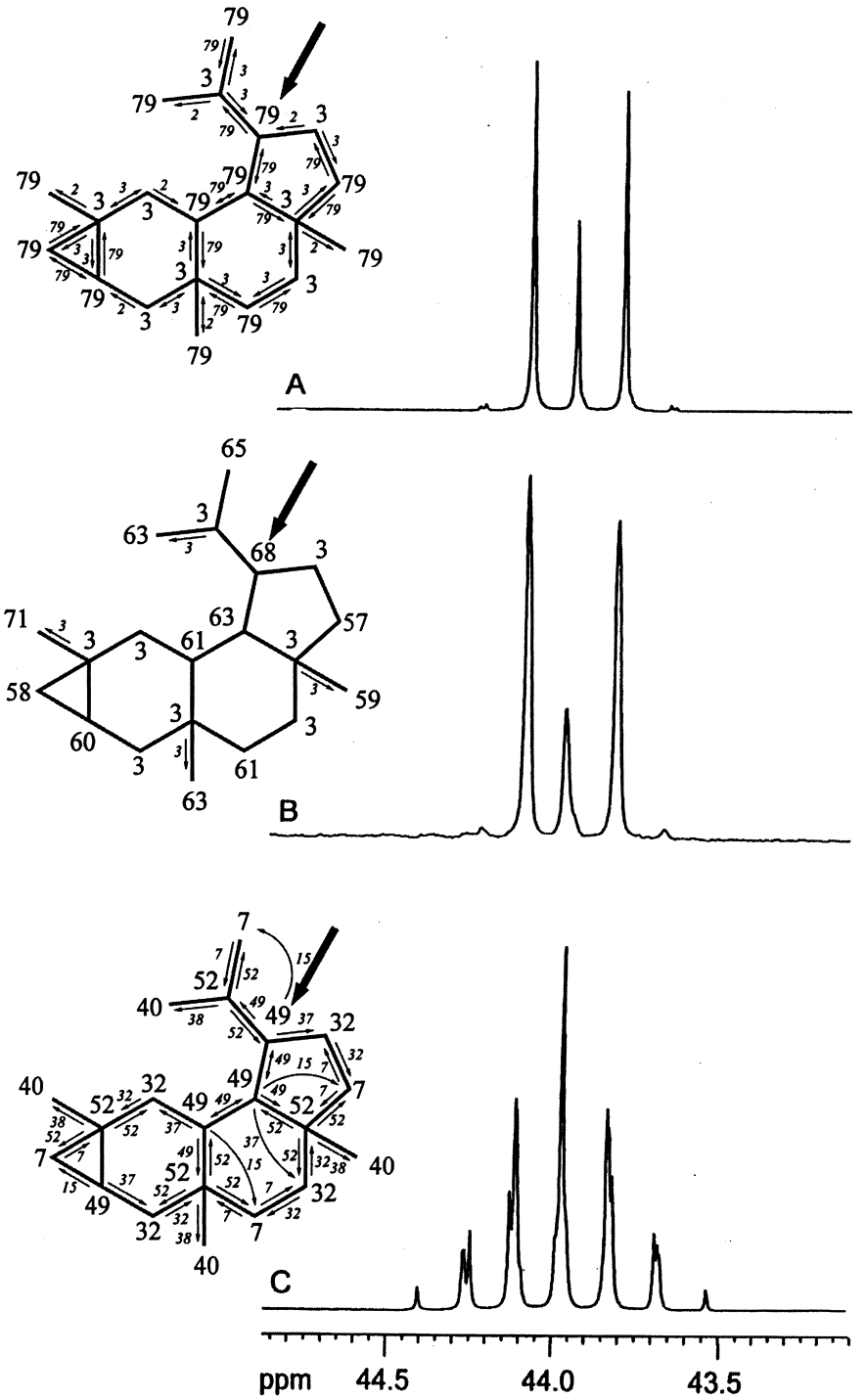

Fig. 10. Observed and predicted labelling patterns for verrucosan-2β-ol and simulated ^{13}C NMR spectra for C-13 (arrow) after feeding with [2-^{13}C]acetate. A: Prediction via the mevalonate pathway. B: Observed. C: Prediction via the deoxyxylulose pathway.

[U-$^{13}C_2$]acetate grown cells indicate that intact two-carbon fragments were transferred to the diterpene without disruption of the CC bond in the original acetate molecule (Fig. 7C). The pairs of jointly transferred two-carbon fragments are visualised even more clearly in the two-dimensional INADEQUATE spectrum shown in Fig. 7H, where they are indicated by bold lines connecting the respective signals.

Experiments were also performed with [1-$^{13}C_1$]- or [2-$^{13}C_1$]acetate as supplement. In this case, the ^{13}C-labelled acetate samples were added as a bolus resulting in a rapid switch from autotrophic to heterotrophic metabolism [6]. The verrucosan-2β-ol carbon atoms labelled in these experiments are indicated by blue circles for [2-$^{13}C_1$]acetate and by green circles for [1-$^{13}C_1$]acetate (Fig. 7B). It is immediately obvious that the label distribution in the two samples is mutually exclusive. As a consequence of the bolus feeding, the intermediary metabolism of the microorganism was flooded with acetate. Somewhat surprisingly, this resulted into substantial $^{13}C^{13}C$ coupling in the ^{13}C spectra of verrucosan-2β-ol which indicates the presence of isotopomers with ^{13}C labelling in directly adjacent positions (Fig. 7F). This is unexpected since each precursor molecule imported only one single ^{13}C atom. A more detailed analysis reveals that the multiply labelled verrucosan-2β-ol isotopomers result from the incorporation of several ^{13}C-labelled acetate molecules into a single verrucosan-2β-ol molecule. In other words, the stochastic recombination of the singly ^{13}C-labelled precursor molecules is responsible for the multiply, ^{13}C-labelled isotopomers.

This example emphasises the influence of the specific feeding strategy. It is shown to exemplify some of the pitfalls in the setup and interpretation of labelling experiments.

On the basis of the labelling patterns in Fig. 7B,C, three of the four isoprenoid units incorporated into the diterpene could be dissected out (Fig. 7D). It is immediately obvious that the C5 unit shown in green must represent the outcome of the reshuffling of an isoprenoid unit caused by a rearrangement reaction. It is also obvious from the pattern in Fig. 7C that seven acetate moieties had been incorporated intact into the diterpene whereas one acetate unit had been disrupted by the rearrangement reaction mentioned above.

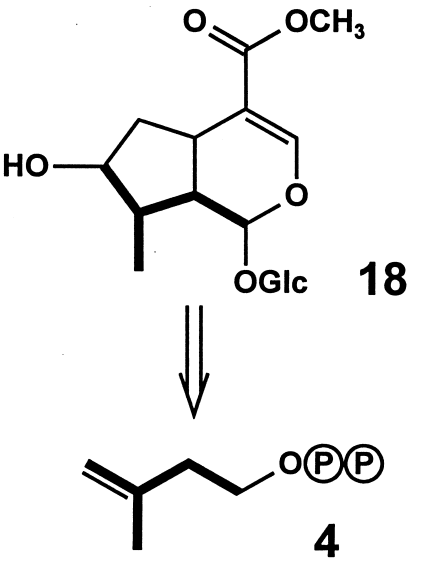

Fig. 11. Reconstruction of IPP (**4**) labelling patterns from loganin (**18**).

Based on these data, the complex sequence of reactions involved in the formation of the tetracyclic diterpenes could be unravelled (Fig. 8). Solvolysis of the allylic pyrophosphate group of (*S*)-geranyllinaloyl pyrophosphate (**10**) triggers off a cyclisation process leading via the monocyclic intermediate (**11**) to the bicyclic ionic intermediate (**12**). The *S* configuration of the precursor can be predicted from the configuration of the chiral centre in intermediate (**11**) and the known anti-stereochemistry of similar $S_{N2'}$ bond-making processes [37,38]. Next, ion **12** suffers a 1,2-rearrangement leading to intermediate **13**, the cationic centre of which then attacks the isopropylidene double bond with formation of the tricyclic ion (**14**). Saturation of the positive charge in this ion is best accommodated by a 1,5-hydride transfer from the C-2 methylene group which generates the homoallylic intermediate (**15**). Similar shifts have been observed previously in terpene biosynthesis [39,40]. Collapse of intermediate **15** to the cyclopropylcarbinyl ion (**16**) is followed by a sigmatropic rearrangement to a new cyclopropylcarbinyl ion (**17**) and the reaction is terminated by addition of a hydroxyl group from the solvent. The interconversion of the two cyclopropylcarbinyl ions **16** and **17**, which may but need not require the intermediacy of a cyclobutyl

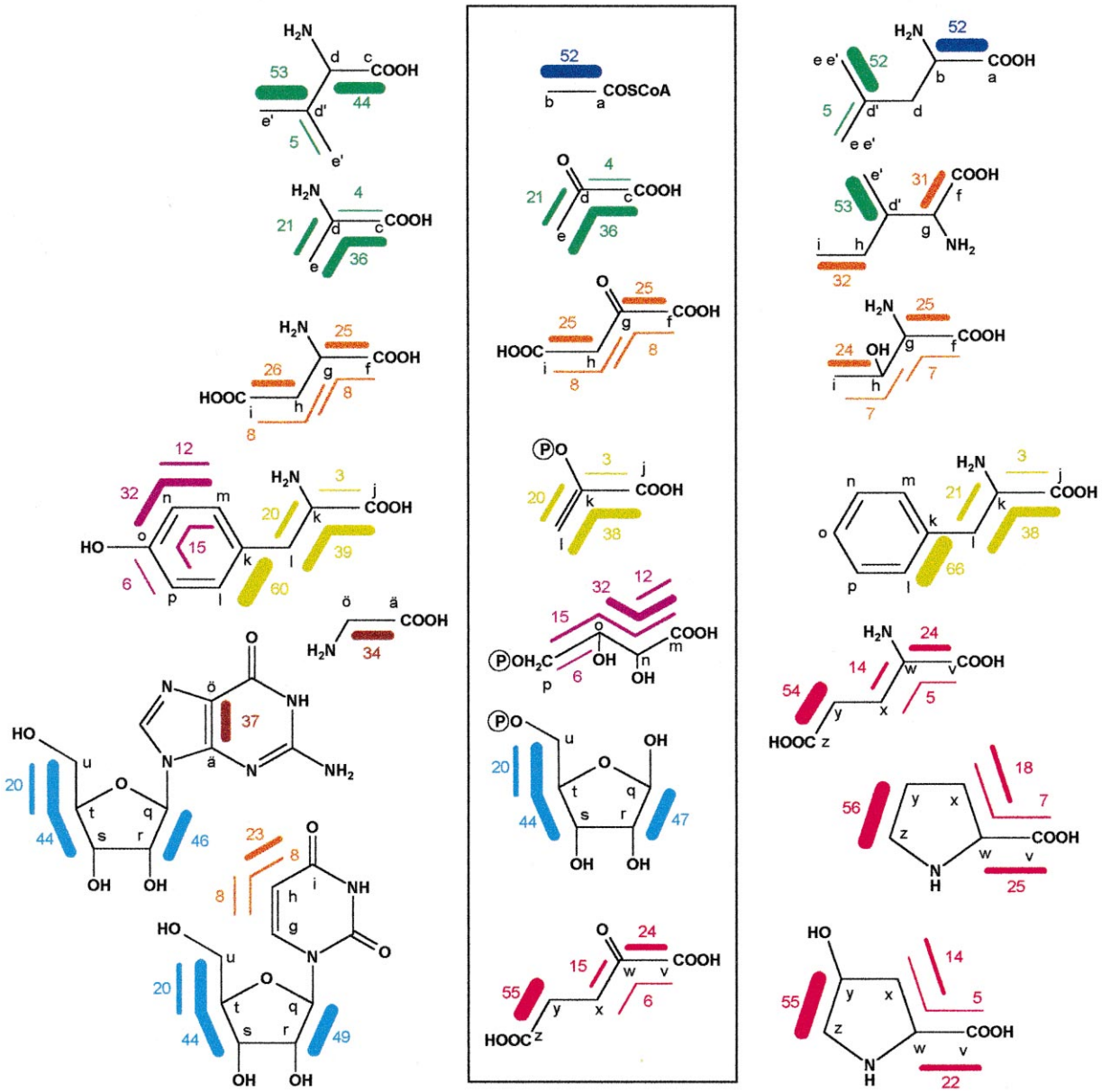

Fig. 12. Labelling patterns of primary metabolites from amino acids and nucleosides after feeding of *Rauwolfia serpentina* cells grown on a mixture of [U-$^{13}C_6$]glucose and unlabelled glucose (1:25; w/w).

cation, is well precedented in abiotic and biological systems [41].

From the labelling patterns of amino acids isolated after hydrolysis of bacterial cell mass, the labelling patterns for the triose pool, the pyruvate pool and the acetyl CoA pool could be reconstructed for each of the labelling experiments [6]. From these results, the hypothetical labelling patterns of isoprenoids via the mevalonate pathway and the 1-deoxy-D-xylulose pathway could be predicted quantitatively. Starting from [2-$^{13}C_1$]acetate as the proffered compound, the predictions for both pathways are com-

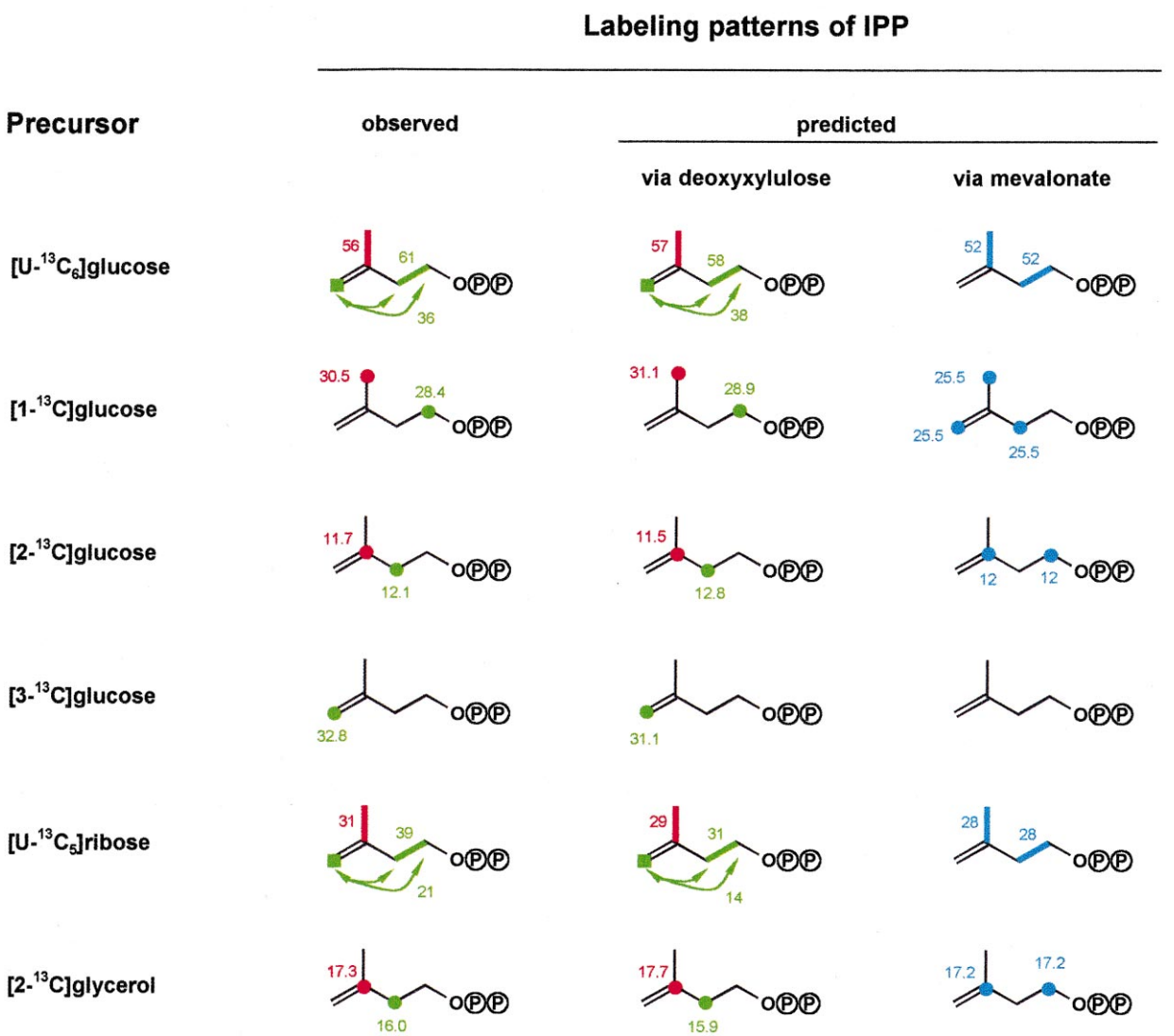

Fig. 13. Labelling patterns of IPP in loganin from a cell culture of *R. serpentina* after feeding with various ^{13}C-labelled carbohydrates.

pared with the experimental labelling data in Fig. 9. The experimental data are in agreement with the mevalonate prediction but not with the 1-deoxy-D-xylulose prediction. The accuracy of the prediction is also illustrated graphically in Fig. 10 which compares the simulated ^{13}C NMR spectra for carbon C-13 of verrucosan-2β-ol via the mevalonate pathway and via the 1-deoxy-D-xylulose pathway with the experimental data for carbon C-13 of verrucosan-2β-ol. Again, it is obvious that only the mevalonate prediction is in line with the experimental findings.

The liverwort *Fossombronia alaskana* produces 8α-acetoxy-13α-hydroxy-5-oxo-*epi*-neoverrucosan, a compound with a carbocyclic skeleton generated from intermediate **16** (Fig. 8). Feeding experiments with various ^{13}C-labelled glucose samples showed that the biosynthesis of the terpene in the plant proceeded via the 1-deoxy-D-xylulose pathway [42].

Table 1
Current knowledge on the occurrence of the alternative pathways for terpenoid biosynthesis

Bacteria	Deoxyxylulose pathway	Mevalonate pathway	Reference
Alicyclobacillus acidoterrestris	Hopanoid		[16]
Caldariella acidophila		Ether lipids	[44]
Chainia rubra		Napyradiomycin	[90]
Chloroflexus aurantiacus		Verrucosanol	[34]
Corynebacterium ammoniagenes	Menaquinone, 2-methyl-D-erythritol		[91,92]
Escherichia coli	Ubiquinone, menaquinone		[16–18,93,94]
Flavobacterium		Zeaxanthin	[95]
Halobacterium cutirubrum		Carotenoids	[96]
Kitasatosporia		Terpentecin	[97]
Methanobacterium thermoautotrophicum		Ether lipids	[44]
Methylobacterium fujisawaense	Ubiquinone, hopanoids		[16]
Methylobacterium organophilum	Hopanoids		[98]
Rhodopseudomonas palustris	Hopanoids		[98]
Rhodopseudomonas acidophila	Hopanoids		[98]
Streptomyces aeriouvifer	Menaquinone	Furachinocin, naphterpin	[99–101]
Streptomyces spheroides	Novobiocin		[102]
Streptomyces sp.	Pentalenolactone		[103]
Synechocystis sp.	Phytol, β-carotene		[50]
Zymomonas mobilis	Hopanoid		[16]
Plants			
Catharanthus roseus	β-Carotene, phytol, lutein	Sitosterol	[45]
Chelidonium majus	Isoprene		[104]
Chlamydomonas reinhardtii	Phytol, ergosterol, 7-dehydroporiferasterol		[104]
Conocephalum conicum	Bornyl acetate		[105]
Cyanidium caldarium	Phytol	Ergosterol	[104]
Daucus carota	Phytol	Sitosterol, stigmasterol	[106]
Euglena gracilis		Sterols, phytol	[50]
Fossombronia alaskana	Epineoverrucosane		[42]
Ginkgo biloba	Ginkgolide A	Sitosterol	[19]
Heteroscyphus planus	Phytol	β-Carotene, phytol, heteroscyphic acid A	[107–109]
Hordeum vulgare	β-Carotene, phytol, plastoquinone	Sitosterol, stigmasterol	[106]
Ipomoea parasitica	2-C-Methyl-D-erythritol		[110]
Lemna gibba	β-Carotene, phytol, plastoquinone, lutein	Sitosterol, stigmasterol	[104,106]
Liriodendron tulipifera	2-C-Methyl-D-erythritol		[110]
Lithospermum erythrorhizon		Shikonin	[112]
Lococolea heterophylla		β-Carotene, phytol	[108]
Marrubium vulgare	Marrubiin		[113]
Mentha piperita	Menthone		[111,114]
Mentha pulegium	Pulegone		[111,114]
Morus alba		Sitosterol	[115]
Nicotiana tabacum	Plastoquinone	Sterols, ubiquinone	[48]
Pelargonium graveoleus	Geraniol		[111,114]
Populus nigra	Isoprene		[104]
Rauwolfia serpentina	Loganin		[8,116]
Ricciocarpos natans		Ricciocarpin A	[105]
Rubia tinctorum	Lucidin-3β-primveroside, rubiadin-3β-primveroside		[8]
Salix viminalis	Isoprene		[104]
Salvia miltiorrhiza	Ferruginol		[117]
Scenedesmus obliquus	Phytol, plastoquinone, β-carotene, lutein, chondrillasterol, ergost-7-enol		[104,118]
Taxus chinensis	Taxuyunnanine C		[10]
Thymus vulgaris	Thymol		[111,114]

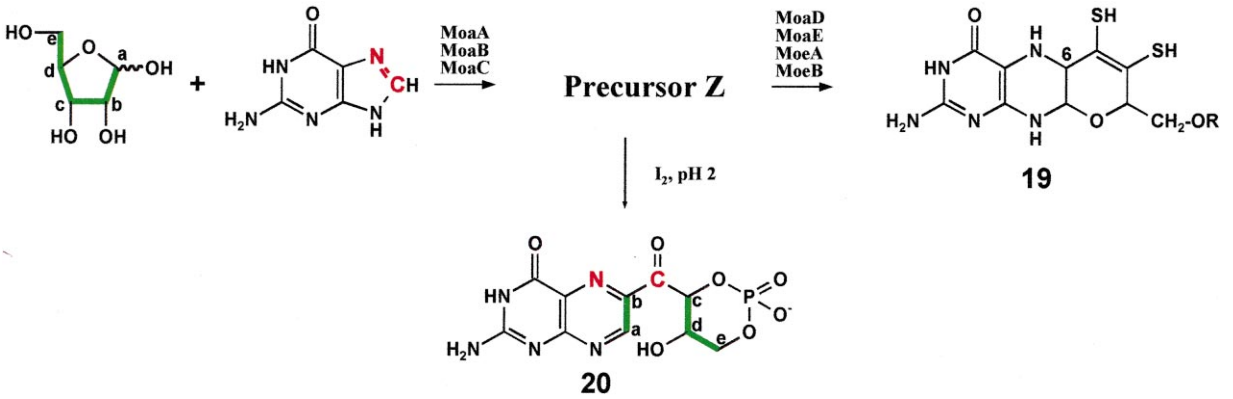

Fig. 14. Conversion of a guanine derivative to molybdopterin via precursor Z. Precursor Z can be converted to the stable Compound Z. The distribution of carbon atoms after feeding of [U-$^{13}C_5$]ribulose 5-phosphate is shown in green, and of [7-^{15}N,8-^{13}C]guanine is shown in red. MoaA, MoaB, MoaC, MoaD, MoaE, MoeA and MoeB are proteins assumed to be involved in the biosynthesis of molybdopterin (**19**) [119,120].

4. Biosynthesis of the monoterpene loganin in *Rauwolfia serpentina*

The monoterpene loganin (**18**) (Fig. 11) is a biosynthetic precursor of numerous indole alkaloids. Experiments carried out with *Menyanthes trifoliata* showed that [2-^{14}C]mevalonate was incorporated into triterpenes and sterols but not into the monoterpene glycoside loganin [43]. Its biosynthesis in cell cultures of the plant *R. serpentina* is described below to illustrate the outcome of retrobiosynthesis experiments using different ^{13}C-labelled precursors. It will also serve to illustrate the reliability of the quantitative prediction of labelling patterns on basis of central intermediates.

Cells of *R. serpentina* were grown with ^{13}C-labelled samples of glucose, ribose or glycerol [9]. Fig. 12 shows that the labelling patterns of amino acids obtained in the experiment with [U-$^{13}C_6$]glucose which can be used to reconstruct labelling patterns of central metabolites. These data can subsequently be used to predict hypothetical labelling patterns for formation of isoprenoid precursors via the mevalonate and the 1-deoxy-D-xylulose pathway. On the basis of the established cyclisation mechanism conducive to iridoid formation, the labelling pattern of IPP (**4**) is easily gleaned from loganin carbon atoms, as shown in Fig. 11. Comparison between the experimental IPP pattern and the predicted labelling patterns are shown for all ^{13}C-labelled precursors used in Fig. 13. The experimental IPP data show close agreement with the 1-deoxy-D-xylulose prediction but not with the mevalonate prediction. These data leave no doubt that loganin is biosynthesised via the 1-deoxy-D-xylulose pathway, although earlier experiments with ^{14}C-labelled precursors had been interpreted in terms of a bulk mevalonoid origin (for review see [12]).

The data in Fig. 13 illustrate that the retrobiosynthetic analysis can be performed with a wide variety of general metabolic precursors. They also show that the agreement between predicted and experimentally determined value is excellent. A more detailed analysis also indicates that [1-$^{13}C_1$]glucose and [U-$^{13}C_6$]glucose are the optimum precursors for the discrimination between the two isoprenoid pathways. In retrospect, it is clear that these two precursors afford isotopomer populations of acetyl CoA, pyruvate, and triose phosphates which are particularly appropriate for this discrimination. The importance of generating the most appropriate isotopomer constellations by an optimised tracer strategy will become even more obvious in the studies on the biosynthesis of molybdopterin described below.

5. Taxonomy of the isoprenoid pathways

As yet, no exceptions to the operation of the mevalonate pathway have been reported in yeasts and

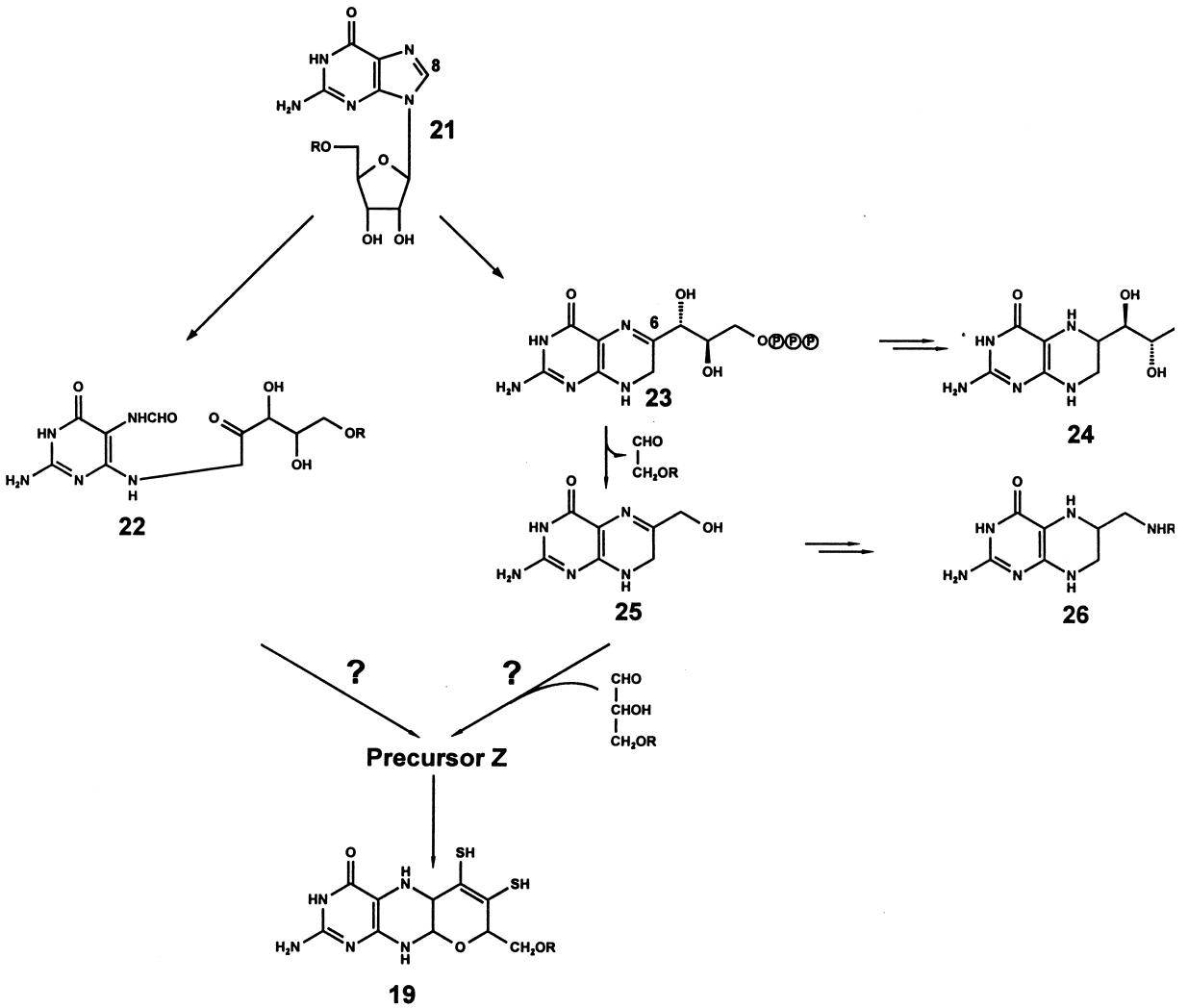

Fig. 15. Pathways proposed in the literature for biosynthetic formation of the carbon skeleton of molybdopterin, via the folic acid (**26**) and biopterin (**24**) biosynthesis intermediates 7,8-dihydroneopterintriphosphate (**23**) and 6-hydroxymethyldihydropterin (**25**) [66] or by fragmentation and reutilisation of the ribose side chain [67].

animals. The mevalonate pathway and the 1-deoxy-D-xylulose pathway have been shown to occur alternatively in different bacteria (Table 1). More specifically, the mevalonate pathway has been demonstrated in the primitive eubacterium, *C. aurantiacus*, and in methanogenic bacteria [34,44]. The 1-deoxy-D-xylulose pathway has been shown to operate in a variety of other eubacteria (Table 1). A final assessment of the distribution of the two pathways in different eubacterial phyla is not yet possible.

In plants, the mevalonate pathway has been shown to be operative in the cytoplasmic compartment where it is responsible for the biosynthesis of sterols [12,45–47]. Recent data also show that ubiquinone of plant mitochondria is formed via mevalonate although it is not known whether IPP and DMAPP are synthesised inside the mitochondrion or imported from the cytoplasm [48]. The 1-deoxy-D-xylulose phosphate pathway appears to be operative in chloroplasts where it has been shown to supply building blocks for carotenoids, for the phytol side chain of chlorophyll and for a variety of monoterpenes and

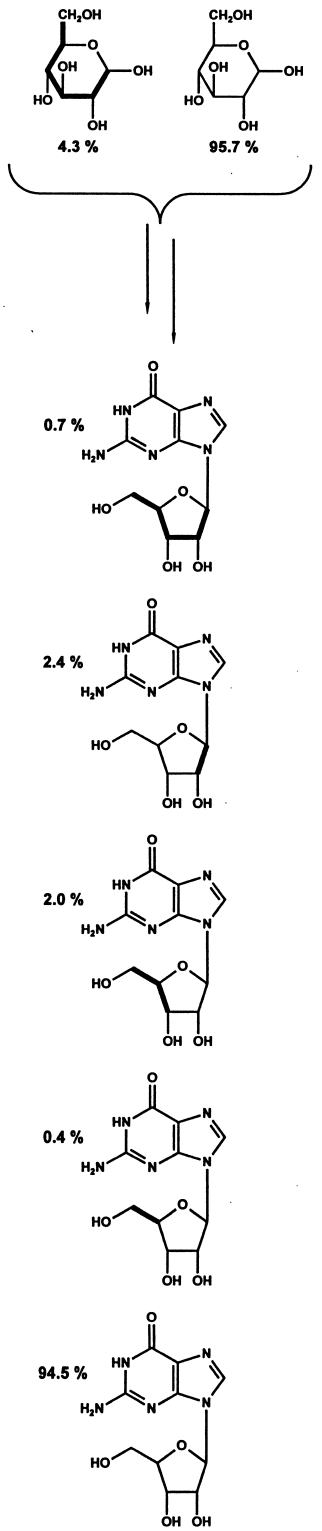

Fig. 16. Relative molar fractions (%) of guanosine isotopomers obtained after feeding a mixture of [U-$^{13}C_6$]glucose and natural abundance glucose to *E. coli*. Bond labelling of the respective isotopomers is shown by bold lines.
←

diterpenes (Table 1) (for review see [15]). The crucial evidence for the existence for the operation of the alternative pathway is best obtained by experiments with ^{13}C-labelled samples of glucose, a metabolite conducive to diversion of label to virtually all plant metabolites.

The compartmental separation of the two isoprenoid pathways in plant cells is not absolute. Mevalonate-derived precursors are incorporated to some extent into 1-deoxy-D-xylulose-derived metabolites and vice versa [45]. This cross-flow may be more prominent in plant cell cultures in vitro than in intact plants.

In retrospect, it is easily understood how numerous researchers had concluded incorrectly that all isoprenoids were universally derived from mevalonate. The experiments had shown that acetate and mevalonate could be diverted to a wide variety of terpenoids in plants, albeit at exceedingly low rates. The low incorporation rates were 'explained away' by different compartments of acetyl CoA as well as other hypotheses, none of which turned out to be correct. The earlier findings are now easily explained by the cross flow of metabolites between the two pathways. However, it should be noted that the precursor species which is exchanged between the cytoplasmic and chloroplast compartment in the plant is still unknown.

The occurrence of two different isoprenoid pathways in different plant compartments may be viewed in terms of the endosymbiont origin of plant cells. Recently, Martin and Müller [49] proposed that eukaryotes could have originated from a methanobacterial organism which had incorporated a eubacterium. This could imply that the cytoplasmic

→

Fig. 17. Relative molar fractions (%) of guanosine and Compound Z isotopomers obtained after feeding a mixture of [U-$^{13}C_5$]ribulose 5-phosphate and natural abundance glucose to *E. coli*. Bond labelling of the respective isotopomer is shown by bold lines.

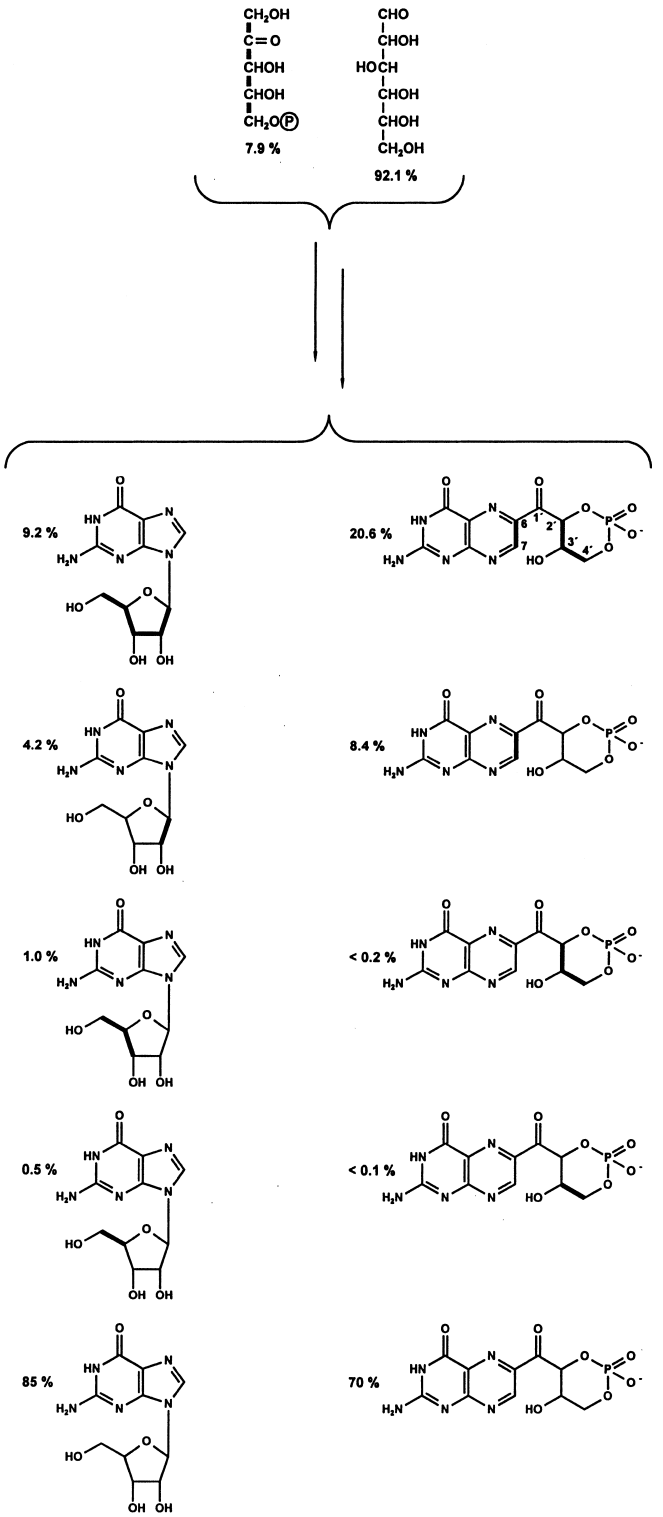
7.9 %
92.1 %
9.2 %
20.6 %
4.2 %
8.4 %
1.0 %
< 0.2 %
0.5 %
< 0.1 %
85 %
70 %

mevalonate enzymes could be the descendant of those of the methanogenic host, whereas the enzyme of the 1-deoxy-D-xylulose pathway may have been derived from a cyanobacterium type endosymbiont. Indeed, cyanobacteria have been shown to utilise the 1-deoxy-D-xylulose pathway [50].

6. Biosynthesis of molybdopterin and of riboflavin

The retrobiosynthetic concept as described above implicates the isolation and NMR analysis of a considerable number of primary metabolites (amino acids and nucleosides). Sometimes, it is sufficient to use the retrobiosynthetic concept at a reduced scale. Thus, it was sufficient to use the labelling patterns of nucleosides but not those of amino acids as a basis of comparison in order to study the biosynthesis of molybdopterin. In earlier studies on riboflavin, it was even sufficient to compare the labelling patterns of different parts of the target molecule. These studies are summarised in Section 7.

Molybdopterin (**19**, Fig. 14) is a cofactor of various redox enzymes, e.g. xanthine dehydrogenase and sulfite oxidase. Biochemical data suggested a dihydropteridine structure with a 4-carbon side chain at position 6 [51]. More recent crystallographic data support a tricyclic structure indicated in Fig. 14 [52–56]. Molybdopterin and its biosynthetic intermediates are unstable. However, an oxidation product of an intermediate designated Compound Z (**20**, Fig. 14) can be isolated from cultures of *moeA* mutants of *E. coli*. Tracer experiments were analysed at the level of Compound Z [57].

Whereas the biosynthesis of molybdopterin is poorly understood, the biosynthetic pathway of the pteridine derivatives tetrahydrofolate (**26**) and tetrahydrobiopterin (**24**) has been studied in considerable detail [58,59]. The first committed precursor for these coenzymes has been shown to be dihydroneopterin triphosphate (**23**) which is obtained from GTP (**21**) by GTP cyclohydrolase I catalysing a mechanistically complex reaction (Fig. 15) [60–65]. Studies by Irby and Adair [66] suggested that dihydroneopterin triphosphate could also serve as a precursor for molybdopterin. Since dihydroneopterin triphosphate carries a three-carbon side chain in position 6, this would imply the introduction of an additional carbon atom. Irby and Adair [66] have suggested that this could occur via the tetrahydrofolate precursor, 6-hydroxymethyldihydropterin (**25**), which is formed by an aldolase type cleavage of dihydroneopterin. An aldol addition of a three-carbon moiety such as glyceraldehyde 3-phosphate (**7**) could then yield an intermediate with the required number of carbon atoms. On the other hand, Wuebbens and Rajagopalan [67] proposed on the basis of studies with ^{14}C-labelled guanosine samples that carbon atom C-8 of the imidazole ring of guanosine is reutilised to increase the length of the position 6 side chain.

In order to discriminate between these hypotheses by retrobiosynthetic analysis, it appeared sufficient to compare the labelling patterns of molybdopterin with those of guanosine and adenosine. As shown in more detail below, it was mandatory to develop a feeding strategy conducive to the intracellular formation of [U-$^{13}C_5$]-labelled pentoses. Originally, it was expected that this could be easily achieved by feeding of [U-$^{13}C_6$]glucose which might be in part converted to the pentose pool by oxidative decarboxylation.

The labelling pattern of the pentose pool is easily assessed by analysis of nucleosides (Fig. 16). Surprisingly, it turned out that *E. coli*, even under aerobic conditions, generates pentoses from glucose almost exclusively by sugar phosphate interconversions via transaldolase and transketolase catalysed reactions which result in breaking of the bond between carbon atoms 3 and 4 of the original glucose molecule (Fig. 16). However, a sufficient concentration of [U-$^{13}C_5$]pentose phosphate isotopomers could be generated with [U-$^{13}C_5$]ribulose 5-phosphate as precursor [57]. Surprisingly, the unconventional nutrient was absorbed and metabolised by the *E. coli* cells with high efficiency.

The labelling patterns of the pentose pool are easily gleaned from Fig. 17. The totally labelled [U-$^{13}C_5$]pentose isotopomer accounts for 9.2 mol %. The isotopomer mixture constituting biosynthetic Compound Z is also shown in Fig. 17. Most important, there was a high abundance of a molecular species with ^{13}C label in carbon atoms 6, 7, 2′, 3′ and 4′. Long range coupling between carbon 6 of the pteridine ring and carbon 2′ of the side chain at position 6 showed unequivocally that a two-carbon fragment and a three-carbon fragment had been incorporated from a single ribulose phosphate mole-

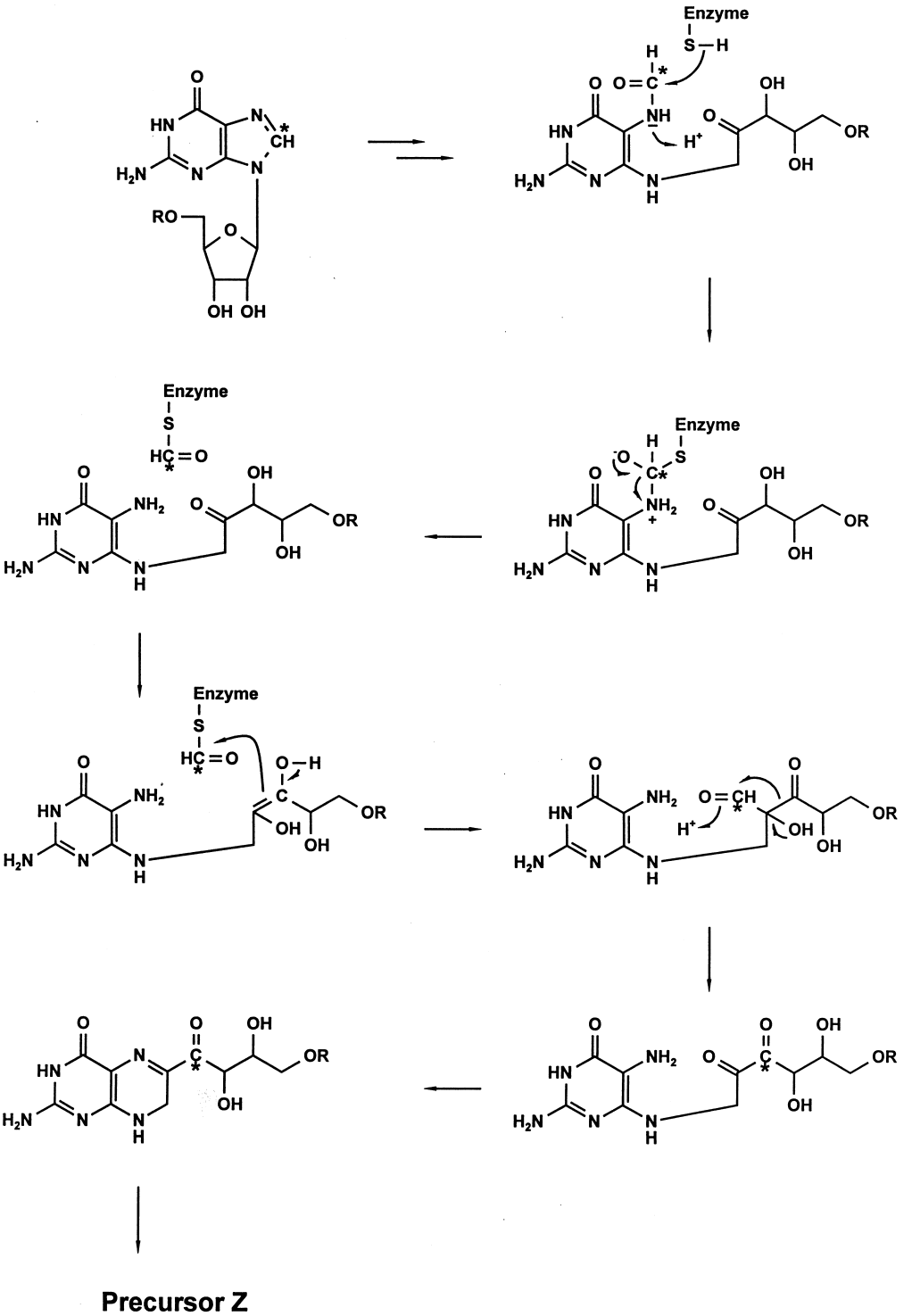

Fig. 18. Hypothetical mechanism for biosynthesis of precursor Z from a guanosine nucleotide (hypothesis I).

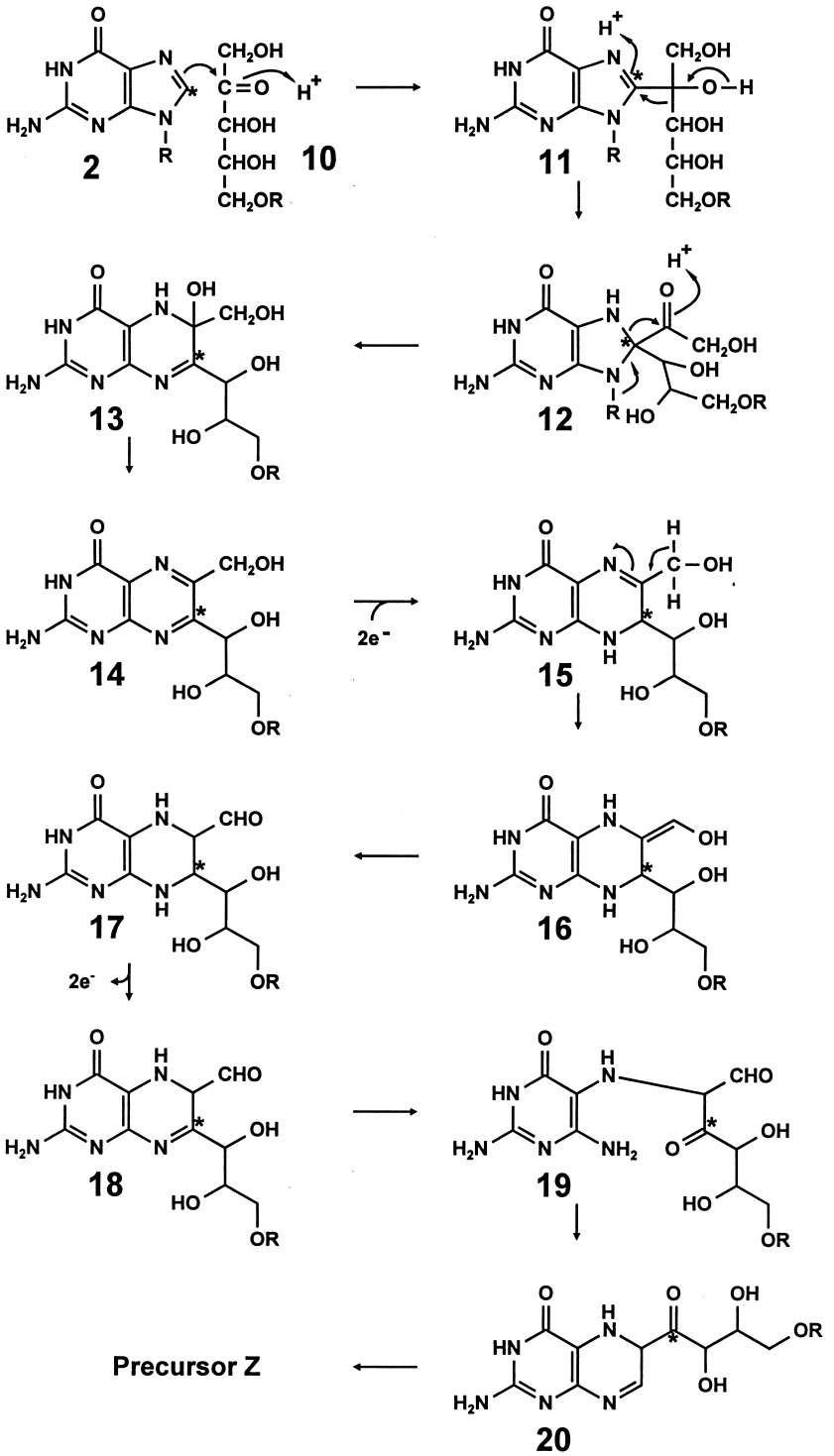

Fig. 19. Hypothetical mechanism for the formation of precursor Z by condensation of a guanine derivative with a ribulose derivative (hypothesis II).

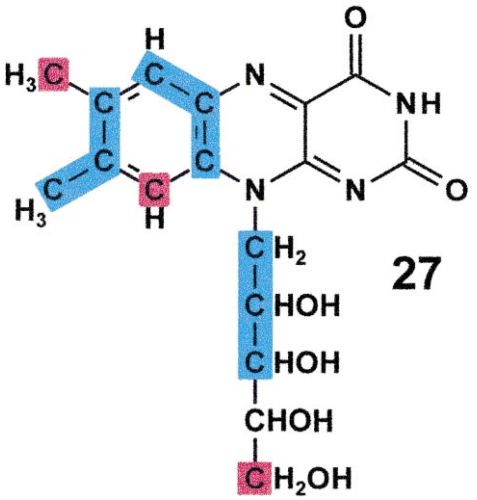

Fig. 20. Labelling pattern of riboflavin samples obtained from a variety of ^{13}C-labelled precursors [68–73]. Colours indicate structural motifs characterised by corresponding labelling patterns.

cule despite the presence of a very large amount of unlabelled glucose. Thus, the pentose moiety had been transformed by an intramolecular rearrangement conducing to the interposition of a 1-carbon fragment between the carbon atoms 2 and 3 of the original pentose.

The origin of the 1-carbon fragment (C-1′ in Compound Z) was addressed using [7-^{15}N,8-^{13}C]guanine as a precursor [57]. Not surprisingly, the double labelled guanine was incorporated into the guanine and the adenine nucleotide pools without changes in the ring skeleton (i.e. conservation of 'bond labelling' between nitrogen-7 and carbon-8 of the imidazole ring). In Compound Z, the bond between these two atoms had been broken, but the two labelled atoms have been reunited by an intramolecular rearrangement, thus affording Compound Z with ^{15}N in position 5 and ^{13}C in position 1′ (Fig. 14).

Hypothetical mechanisms in line with these experimental findings are shown in Figs. 18 and 19. It should be noted that all the hypothetical reaction steps have chemical and biochemical precedent. A more detailed discussion of these mechanisms has been published elsewhere [57]. For the purpose of the present review we would like to emphasise that this complex biochemical pathway involving two intramolecular rearrangement steps could be addressed by the retrobiosynthetic concept, even in the shortcut form where only selected primary metabolites are used for comparison.

We will now briefly discuss some older experiments where the retrobiosynthetic concept could be used in an even more abbreviated form, namely by comparing the labelling patterns of different parts of a target molecule using a variety of differently ^{13}C-labelled precursors. It has been known since several decades that the ribityl side chain of the vitamin, riboflavin (**27**, Fig. 20), originates by reduction of the ribose moiety incorporated from the precursor, GTP (for review see [68]). It was also well known that the xylene ring of the isoalloxazine moiety is assembled from two identical four-carbon moieties. However, the nature of that four-carbon moiety had resisted elucidation.

In experiments using a variety of ^{13}C-labelled carbohydrates it was shown that the labelling pattern of the elusive four-carbon precursor invariably reflected the labelling pattern of carbon atoms 1′, 2′, 3′ and 5′ of the ribityl side chain of the vitamin (Fig. 20) [69–73]. Moreover, the experiments showed that the four-carbon precursor had been formed by the loss of C-4 of a pentose type precursor with subsequent

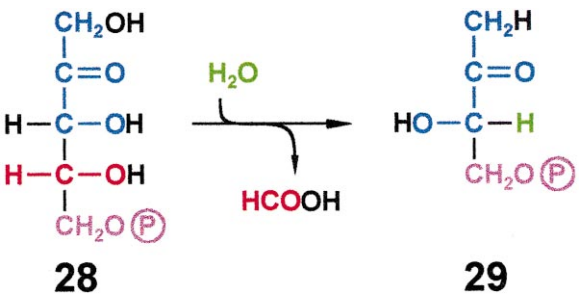

Fig. 21. Atom transfer map for the enzyme-catalysed formation of 3,4-dihydroxy-2-butanone 4-phosphate [68–73].

reconnection of C-5 with C-3 through an intramolecular rearrangement (Fig. 21).

On the basis of these data it became possible to identify the four-carbon unit as 3,4-dihydroxy-2-butanone 4-phosphate (**29**) and to show by in vitro experiments that it was obtained from ribulose 5-phosphate (**28**) by the unusual reaction mechanism shown in Fig. 22 [69–73]. It should be noted that this reaction sequence involves the elimination of C-4 of the pentulose phosphate chain as formate, a reaction sequence which is essentially the reverse of the formate interposition observed in the formation of Compound Z (see above). In retrospect, it may be added that the retrobiosynthetic concept actually originated as an extension of the riboflavin experiments by inclusion of a progressively larger number of metabolite species for the pattern recognition approach.

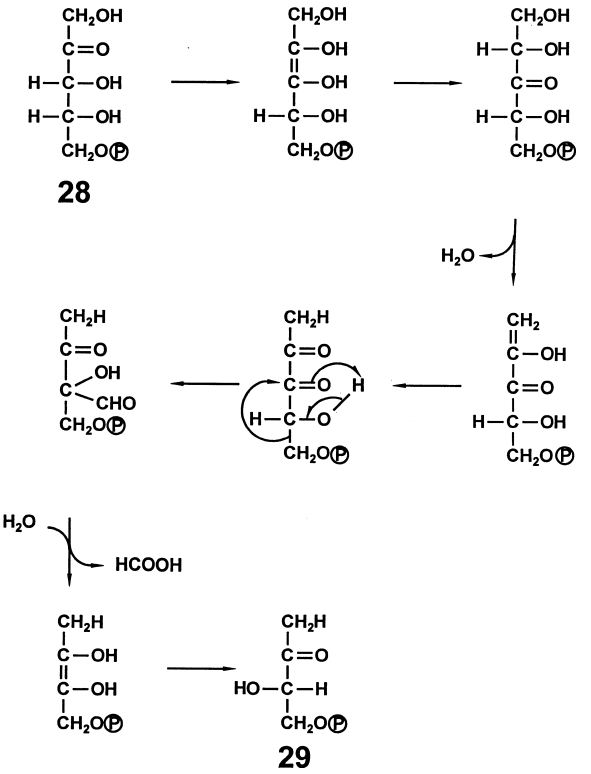

Fig. 22. Hypothetical mechanism for the formation of 3,4-dihydroxy-2-butanone 4-phosphate [67–72].

7. Analysis of carbon fixation pathways

Knowledge of the metabolic pathways used for the biosynthesis of individual amino acids is required in order to reconstruct the labelling of central intermediate pools. Tryptophan, phenylalanine and tyrosine are universally formed via the shikimate/chorismate pathway in all organisms capable of their synthesis. Most other amino acids can be obtained via more than one pathway. In order to apply the retrobiosynthetic concept, the pathways used in the organism under study must be determined as part of the study unless it has already been established in earlier experiments with a high degree of certainty. To make matters worse, a given amino acid is sometimes formed via more than one pathway in the same organism. In those cases, we are faced with the additional task of determining the partitioning between the different pathways. As mentioned above, these multiple tasks can be solved by the same approach since the experimental system is substantially overdetermined if all amino acid labelling patterns have been detected with high precision in experiments with several different isotope-labelled compounds or different isotopomers of the same compound.

Recent studies have shown that the central metabolic flux patterns in different plants are surprisingly similar (Bacher, Eisenreich, Zenk, Rieder, Eichinger, Werner, unpublished data; [7,74]). On the other hand, the central metabolic patterns as well as the amino acid biosynthetic pathways show considerable variability in different microorganisms. As an example, the CO_2 fixation pathways in two strictly anaerobic bacteria are summarised below.

In bacteria, four pathways of auxotrophic CO_2 fixation have been observed, i.e. (i) the reductive pentose phosphate cycle, (ii) the reductive citrate cycle, (iii) the reductive acetyl CoA/carbon monoxide dehydrogenase pathway, and (iv) the 3-hydroxypropionate pathway (for review see [75]). The latter pathway had been proposed to operate in the primitive eubacterium *C. aurantiacus* by Holo and coworkers [76–78]. The retrobiosynthetic analysis of the amino acid pathways in this microorganism have been described elsewhere and will not be discussed in detail [6,79].

On basis of the labelling patterns of the central metabolic intermediates, the metabolic cycle designated A in Fig. 23 could be established [6]. Briefly,

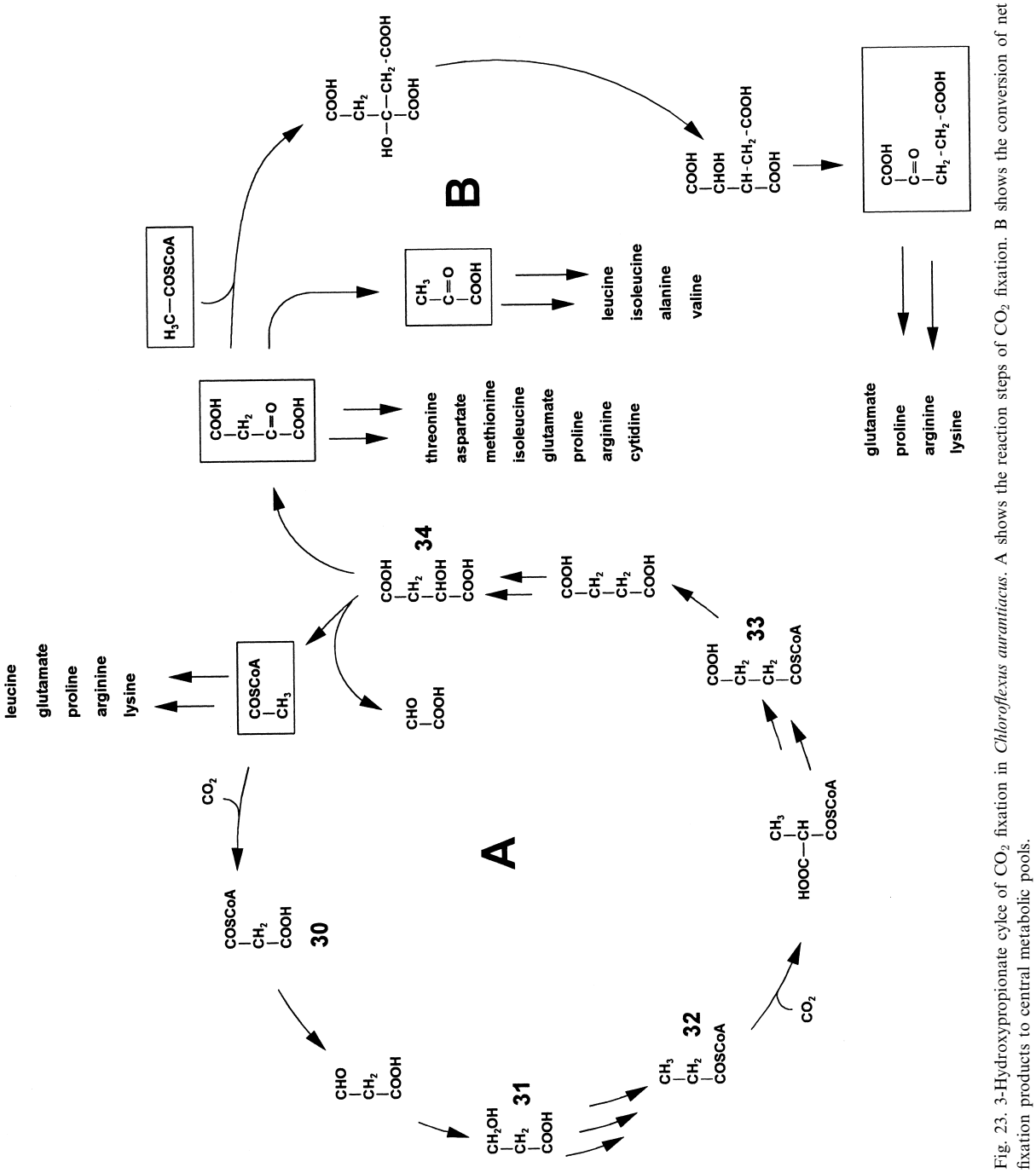

Fig. 23. 3-Hydroxypropionate cylce of CO_2 fixation in *Chloroflexus aurantiacus*. A shows the reaction steps of CO_2 fixation. B shows the conversion of net fixation products to central metabolic pools.

it was shown that CO_2 is originally fixed by formation of malonyl CoA (**30**) from acetyl CoA (**2**). Reduction of the thioester group affords 3-hydroxypropionate (**31**) which can be isolated in relatively large quantity. All required enzyme activities for a respective CO_2 fixation have been determined in vitro [80].

3-Hydroxypropionate is subsequently converted into its CoA ester and then to succinyl-CoA (**33**) by a sequence of dehydration, reduction, carboxylation and rearrangement steps (Fig. 23). The cleavage of malate (**34**) regenerates acetyl CoA (**2**) which is consumed in the initial CO_2 fixation steps. Intermediates of the pathway are diverted to various anabolic pathways where they serve as precursors for amino acids and other cellular constituents (Fig. 23B).

Meanwhile the 3-hydroxypropionate pathway has been assumed to be operative in the facultative anaerobic thermoacidophilic archaebacterium *Acidianus brierleyi* [81]. In *A. brierleyi* cells growing autotrophically, the key enzymes of the 3-hydroxypropionate cycle, acetyl-CoA carboxylase and propionyl-CoA carboxylase have been determined, while ATP citrate lyase, the key enzyme of the reductive tricarboxylic acid cycle could not be detected.

Using a similar strategy with ^{13}C-labelled succinate as precursor, it could be shown that CO_2 fixation proceeds via the reductive citrate cycle in *Thermoproteus neutrophilus* [6,79,82]. The enzyme ATP citrate lyase has a central role in this biosynthetic cycle. Surprisingly, the study showed that this enzyme catalysed the forward as well as the reverse reaction at a high rate even under conditions where the net metabolite flux was in the direction of citrate formation. It follows that the intracellular concentration of the enzyme product, citrate, must be high enough to allow for significant reverse flux in the pathway [6,79,82].

8. Metabolic flux in biotechnological processes

Studies of metabolic flux can be important in order to diagnose metabolic bottlenecks in organisms used for biotechnological processes. For example, Wüthrich, Bailey and their coworkers used fermentations with [U-$^{13}C_6$]glucose to diagnose the metabolite flux through the pentose phosphate and the glycolytic cycle in a recombinant strain of *Bacillus subtilis* used for production of riboflavin by fermentation [83]. As described above, most of the carbon atoms for the biosynthesis of the vitamin are supplied as pentose and pentulose phosphate, respectively. Engineering the central metabolic flux in order to channel the carbon flux in the direction of the desired metabolite could help to improve fermentations yield. Similar studies have been reported for other fermentation processes [84–89].

9. Conclusions

The retroanalytic methods described in this paper are more laborious than conventional radioisotope tracer techniques. On the other hand, they yield an abundance of metabolic information and avoid possible pitfalls.

Acknowledgments

This work was supported by grants from the Deutsche Forschungsgemeinschaft (Schwerpunkt 'Neuartige Reaktionen und Katalysemechanismen bei anaeroben Mikroorganismen' and SFB 369 'Molekulare und bioorganische Grundlagen des Sekundärstoffwechsels'), in part by the EC Grant ERBCHRXCT 930243 and by the Fonds der Chemischen Industrie. We thank Prof. H. Simon for helpful discussions.

References

[1] Schönheimer, R. and Rittenberg, D. (1935) Deuterium as an indicator in the study of intermediary metabolism. Science 82, 156–157.
[2] Kamen, M.D. (1947) Use of isotopes in biochemical research: Fundamental aspects. Annu. Rev. Biochem. 16, 631–654.
[3] Calvin, M., Heidelberger, C., Reid, J.C., Tolbert, B.M. and Yankwich, P.F. (1949) Isotopic Carbon. J. Wiley and Sons, New York, Chapman and Hall, London.
[4] Simon, H. and Floss, H.G. (1967) Anwendung von Isotopen in der Organischen Chemie und Biochemie, Bestimmung der Isotopenverteilung in markierten Verbindungen (Simon, H., Ed.), Volume I, Springer Verlag, Berlin.
[5] Rauschenbach, P., Schmidt, H.L., Simon, H., Tykva, R. and

Wenzel, M. (1974) Messung von radioaktiven und stabilen Isotopen (Simon, H., Ed.), Springer Verlag, Berlin.
[6] Eisenreich, W., Strauß, G., Werz, U., Fuchs, G. and Bacher, A. (1993) Retrobiosynthetic analysis of carbon fixation in the phototrophic eubacterium *Chloroflexus aurantiacus*. Eur. J. Biochem. 215, 619–632.
[7] Werner, I., Bacher, A. and Eisenreich, W. (1997) Retrobiosynthetic NMR studies with ^{13}C-labeled glucose. Formation of gallic acid in plants and fungi. J. Biol. Chem. 272, 25474–25482.
[8] Eichinger, D. (1997) Retroanalytische NMR-Untersuchungen zur Biosynthese der Indolalkaloidvorstufe Loganin und von Anthrachinonglykosiden in höheren Pflanzen. Thesis, Technische Universität, Munich.
[9] Eichinger, D., Eisenreich, W., Zenk, M.H. and Bacher, A. (1998) Biosynthesis of loganin via the 1-deoxy-D-xylulose pathway in a cell culture of *Rauwolfia serpentina* (submitted for publication).
[10] Eisenreich, W., Menhard, B., Hylands, P.J., Zenk, M.H. and Bacher, A. (1996) Studies on the biosynthesis of taxol: The taxan carbon skeleton is not of mevalonoid origin. Proc. Natl. Acad. Sci. USA 93, 6431–6436.
[11] Qureshi, N. and Porter, J.W. (1981) Conversion of acetyl-coenzyme A to isopentenyl pyrophosphate. In: Biosynthesis of Isoprenoid Compounds (Porter, J.W. and Spurgeon, S.L., Eds.), Vol. 1, pp. 47–94, John Wiley, New York.
[12] Banthorpe, D.V., Charlwood, B.V. and Francis, M.J.O. (1972) The biosynthesis of monoterpenes. Chem. Rev. 72, 115–155.
[13] Bach, T.J. (1995) Some aspects of isoprenoid biosynthesis in plants. A review. Lipids 30, 191–202.
[14] Bloch, K. (1992) Sterol molecule: structure, biosynthesis and function. Steroids 57, 378–382.
[15] Eisenreich, W., Schwarz, M., Cartayrade, A., Arigoni, D., Zenk, M.H. and Bacher, A. (1998) The 1-deoxy-D-xylulose pathway of terpenoid biosynthesis in plants and microorganisms. Chem. Biol. 5, R221–R233.
[16] Rohmer, M., Knani, M., Simonin, P., Sutter, B. and Sahm, H. (1993) Isoprenoid biosynthesis in bacteria: A novel pathway for the early steps leading to isopentenyl diphosphate. Biochem. J. 295, 517–524.
[17] Rohmer, M., Seemann, M., Horbach, S., Bringer-Meyer, S. and Sahm, H. (1996) Glyceraldehyde 3-phosphate and pyruvate as precursors of isoprenic units in an alternative non-mevalonate pathway for terpenoid biosynthesis. J. Am. Chem. Soc. 118, 2564–5266.
[18] Broers, S.T.J. (1994) Über die frühen Stufen der Biosynthese von Isoprenoiden in *Escherichia coli*. Thesis 10978, ETH, Zürich.
[19] Schwarz, M.K. (1994) Terpen-Biosynthese in *Ginkgo biloba*: Eine überraschende Geschichte. Thesis 19051, ETH, Zürich.
[20] White, R.H. (1978) Stable isotope studies on the biosynthesis of the thiazole moiety of thiamin in *Escherichia coli*. Biochemistry 17, 3833–3840.
[21] David, S., Estramareix, B., Fischer, J.-C. and Thérisod, M. (1981) 1-Deoxy-D-threo-2-pentulose: The precursor of the five-carbon chain of the thiazole of thiamine. J. Am. Chem. Soc. 103, 7341–7342.
[22] Himmeldirk, K., Kennedy, I.A., Hill, R.E., Sayer, B.G. and Spenser, I.D. (1996) Biosynthesis of vitamins B_1 and B_6 in *Escherichia coli*: Concurrent incorporation of 1-deoxy-D-xylulose into thiamin (B_1) and pyridoxal (B_6). J. Chem. Soc. Chem. Commun. 1187–1188.
[23] Hill, R.E., Himmeldirk, K., Kennedy, I.A., Panloski, R.M., Sayer, B.G., Wolf, E. and Spenser, I.D. (1996) The biogenetic anatomy of vitamin B_6. A ^{13}C NMR investigation of the biosynthesis of pyridoxol in *Escherichia coli*. J. Biol. Chem. 271, 30426–30435.
[24] Spenser, I.D. and White, R.L. (1997) Biosynthesis of vitamin B_1 (thiamin): An instance of biochemical diversity. Angew. Chem. Int. Ed. Engl. 36, 1032–1046.
[25] Hill, R.E., Sayer, B.G. and Spenser, I.D. (1989) Biosynthesis of vitamin B_6: Incorporation of D-1-deoxy-D-xylulose. J. Am. Chem. Soc. 111, 1916–1917.
[26] Sprenger, G.A., Schörken, U., Wiegert, T., Grolle, S., de-Graaf, A.A., Taylor, S.V., Begley, T.P., Bringer-Meyer, S. and Sahm, H. (1997) Identification of a thiamin-dependent synthase in *Escherichia coli* required for the formation of the 1-deoxy-D-xylulose 5-phosphate precursor to isoprenoids, thiamin, and pyridoxol. Proc. Natl. Acad. Sci. USA 94, 12857–12862.
[27] Lois, L.M., Campos, N., Putra, S.R., Danielsen, K., Rohmer, M. and Boronat, A. (1998) Cloning and characterization of a gene from *Escherichia coli* encoding a transketolase-like enzyme that catalyzes the synthesis of D-1-deoxy-D-xylulose 5-phosphate, a common precursor for isoprenoid, thiamin, and pyridoxol biosynthesis. Proc. Natl. Acad. Sci. USA 95, 2105–2110.
[28] Campos, N., Lois, L.M. and Boronat, A. (1997) Nucleotide sequence of a rice cDNA encoding a transketolase-like protein homologous to the *Arabidopsis* CLA1 gene product. Plant Physiol. 115, 1289.
[29] Lange, B.M., Wildung, M.R., McCaskill, D. and Croteau, R. (1998) A family of transketolases that direct isoprenoid biosynthesis via a mevalonate-independent pathway. Proc. Natl. Acad. Sci. USA 95, 2100–2104.
[30] Yokota, A. and Sasajima, K. (1986) Formation of 1-deoxyketoses by pyruvate dehydrogenase and acetoin dehydrogenase. Agric. Biol. Chem. 50, 2517–2524.
[31] Gibson, J., Ludwig, W., Stackebrandt, E. and Woese, C.R. (1985) The phylogeny of the green photosynthetic bacteria: Absence of a close relationship between *Chlorobicum* and *Chloroflexus*. Syst. Appl. Microbiol. 6, 152–156.
[32] Woese, C.R. (1987) Bacterial evolution. Microbiol. Rev. 51, 227–271.
[33] Oyaizu, W., Debrunner-Vossbrinck, B., Mandelco, L., Studier, J.A. and Woese, C.R. (1987) The green non sulfur bacteria: a deep branching in the eubacterial line of descent. Syst. Appl. Microbiol. 9, 47–53.
[34] Rieder, C., Strauß, G., Fuchs, G., Arigoni, D., Bacher, A. and Eisenreich, W. (1998) Biosynthesis of the diterpene verrucosan-2β-ol in the phototrophic eubacterium *Chloroflexus au-*

rantiacus. A retrobiosynthetic NMR study. J. Biol. Chem. 273, 18099–18108.

[35] Chuck, J.-A. and Barrow, K.D. (1995) The isolation of isoagathenediol: A new tricyclic diterpene from the lipids of *Rhodospirillum rubrum*. Microbiology 141, 2659–2663.

[36] Hefter, J., Richnow, H.H., Fischer, U., Trendel, J.M. and Michaelis, W. (1993) (−)-Verrucosan-2β-ol from the phototrophic bacterium *Chloroflexus aurantiacus*: First report of a verrucosane-type diterpenoid from a prokaryote. J. Gen. Microbiol. 139, 2757–2761.

[37] Godtfredsen, S., Obrecht, J.P. and Arigoni, D. (1977) The cyclization of linalool to α-terpineol. Stereochemical course of the reaction. Chimia 31, 62–63.

[38] Cane, D.E. (1985) Isoprenoid biosynthesis. Stereochemistry of the cyclization of alkylic pyrophosphates. Acc. Chem. Res. 18, 220–226.

[39] Canonica, L., Fiecchi, A., Galli-Kienle, M., Ranzi, B. M. and Scala, A. (1967) The stereochemical course of the 1,5-shift of hydrogen in the biosynthesis of ophiobolus. Tetrahedron Lett. 8, 4657–4659.

[40] Arigoni, D. (1968) Some studies in the biosynthesis of terpenes and related compounds. Pure Appl. Chem. 17, 331–348.

[41] Dauben, W.G. and Friedrich, L.E. (1967) Cyclopropylcarbinyl rearrangements in the thujopsene series. Tetrahedron Lett. 8, 1735–1740.

[42] Eisenreich, W., Rieder, C., Grammes, C., Heßler, G., Adam, K.-P., Becker, H., Arigoni, D., and Bacher, A. (1998) Mechanisms of neoverrucosane formation in the liverwort *Fossombronia alaskana*. A retrobiosynthetic NMR study (manuscript in preparation).

[43] Brechbühler-Bader, S., Coscia, C.J., Loew, P., v. Sczepanski, C. and Arigoni, D. (1968) The chemistry and biosynthesis of loganin. J. Chem. Soc. Chem. Commun. 136–137.

[44] de Rosa, M., Gambacorta, A. and Nicolaus, B. (1980) Regularity of isoprenoid biosynthesis in the ether lipids of archaebacteria. Phytochemistry 19, 791–793.

[45] Arigoni, D., Sagner, S., Latzel, C., Eisenreich, W., Bacher, A. and Zenk, M.H. (1997) Terpenoid biosynthesis from 1-deoxy-D-xylulose in higher plants by intramolecular skeletal rearrangement. Proc. Natl. Acad. Sci. USA 94, 10600–10605.

[46] Goodwin, T.W. (1965) Biochemistry of chloroplasts. In: Chemistry and Biochemistry of Plant Pigments (Goodwin, T.W., Ed.), pp. 143–154. Academic Press, London.

[47] Loomis, W.D. (1967) Biosynthesis and metabolism of monoterpenes. In: Terpenoids in Plants (Pridham, J.B., Ed.), pp. 59–82. Academic Press, London.

[48] Disch, A., Hemmerlin, A., Bach, T.J. and Rohmer, M. (1998) Mevalonate-derived isopentenyl diphosphate is the biosynthetic precursor of ubiquinone prenyl side chain in tobacco BY-2 cells. Biochem. J. 331, 615–621.

[49] Martin, W. and Müller, M. (1998) The hydrogen hypothesis for the first eukaryote. Nature 392, 37–41.

[50] Lichtenthaler, H.K. (1998) Der 1-Desoxy-D-xylulose-Biosyntheseweg pflanzlicher Isoprenoide. Biospektrum 4, 49–52.

[51] Kramer, S.P., Johnson, J.L., Ribeiro, A.A., Millington, D.S. and Rajagopalan, K.V. (1987) The structure of the molybdenum cofactor. Characterization of di(carboxamidomethyl)-molybdopterin from sulfite oxidase and xanthine oxidase. J. Biol. Chem. 262, 16357–16363.

[52] Hille, R. (1996) The mononuclear molybdenum enzymes. Chem. Rev. 96, 2757–2816.

[53] Romão, M.J., Archer, M., Moura, I., Moura, J.J.G., LeGall, J., Engh, R., Schneider, M., Hof, P. and Huber, R. (1995) Crystal structure of the xanthine oxidase-related aldehyde oxido-reductase from *D. gigas*. Science 270, 1170–1176.

[54] Schindelin, H., Kisker, C., Hilton, J., Rajagopalan, K.V. and Rees, D.C. (1996) Crystal structure of DMSO reductase: Redox-linked changes in molybdopterin coordination. Science 272, 1615–1621.

[55] Boyington, J.C., Gladyshev, V.N., Khangulov, S.K., Stadtman, T.C. and Sun, P.D. (1997) Crystal structure of formate dehydrogenase H: Catalysis involving Mo, molybdopterin, selenocysteine, and an Fe_4S_4 cluster. Science 275, 1305–1308.

[56] Chan, M.K., Mukund, S., Kletzin, A., Adams, M.W.W. and Rees, D.C. (1995) Structure of a hyperthermophilic tungstopterin enzyme, aldehyde ferredoxin oxidoreductase. Science 267, 1463–1469.

[57] Rieder, C., Eisenreich, W., O'Brien, J., Richter, G., Götze, E., Boyle, P., Blanchard, S., Bacher, A. and Simon, H. (1998) Rearrangement reactions in the biosynthesis of molybdopterin. An NMR study with multiply $^{13}C/^{15}N$ labelled precursors. Eur. J. Biochem. 255, 24–36.

[58] Green, J.M., Nichols, B.P. and Matthews, R.G. (1996) Folate biosynthesis, reduction and polyglutamylation. In: *Escherichia coli* and *Salmonella*. Cellular and Molecular Biology (Neidhardt, F.C., Ed.), 2nd edn., Vol. 1, pp. 665–673. American Society for Microbiology, Washington, DC.

[59] Nichol, C.A., Lee, C.L., Edelstein, M.P., Chao, J.Y. and Duchs, D.S. (1983) Biosynthesis of tetrahydrobiopterin by de novo and salvage pathways in adrenal medulla extracts, mammalian cell cultures and rat brain in vivo. Proc. Natl. Acad. Sci. USA 80, 1546–1550.

[60] Weygand, F., Simon, H., Dahms, G., Waldschmidt, M., Schliep, H.J. and Wacker, H. (1961) Über die Biogenese des Leucopterins. Angew. Chem. 73, 402–407.

[61] Burg, W.A. and Brown, G.M. (1968) The biosynthesis of folic acid. VIII. Purification and properties of the enzyme that catalyzes the production of formate from carbon atom 8 of guanosine triphosphate. J. Biol. Chem. 243, 2349–2358.

[62] Shiota, T., Palumbo, M.P. and Tsai, L. (1967) A chemically prepared formamidopyrimidine derivative of guanosine triphosphate as a possible intermediate in pteridine biosynthesis. J. Biol. Chem. 242, 1961–1969.

[63] Shiota, T., Baugh, C.M. and Myrick, J. (1969) The assignment of structure of the formamidopyrimidine nucleoside triphosphate precursor of pteridines. Biochim. Biophys. Acta 192, 205–210.

[64] Nar, H., Huber, R., Auerbach, G., Fischer, M., Hösl, C., Ritz, H., Bracher, A., Meining, W., Eberhardt, S. and Bacher, A. (1995) Active site topology and reaction mechanism of GTP cyclohydrolase I. Proc. Natl. Acad. Sci. USA 92, 12120–12125.

[65] Bracher, A., Eisenreich, W., Schramek, N., Ritz, H., Götze, E., Hermann, A. and Bacher, A. (1998) Biosynthesis of pter-

idines. NMR studies on the reaction mechanism of GTP cyclohydrolase I, pyruvoyltetrahydropterin synthase and sepiapterin reductase. J. Biol. Chem. 273, 28132–28141.

[66] Irby, R.B. and Adair, W.L. Jr. (1994) Intermediates in the folic acid biosynthetic pathway are incorporated into molybdopterin in the yeast, *Pichia canadensis*. J. Biol. Chem. 269, 23981–23987.

[67] Wuebbens, M.M. and Rajagopalan, K.V. (1995) Investigation of the early steps of molybdopterin biosynthesis in *Escherichia coli* through the use of in vivo labeling studies. J. Biol. Chem. 270, 1082–1087.

[68] Bacher, A., Eberhardt, S. and Richter, G. (1996) Biosynthesis of riboflavin. In: *Escherichia coli* and *Salmonella*. Cellular and Molecular Biology (Neidhardt, F.C., Ed.), 2nd edn., Vol. 1, pp. 657–664. American Society for Microbiology, Washington, DC.

[69] Bacher, A., LeVan, Q., Keller, P.J. and Floss, H.G. (1983) Biosynthesis of riboflavin. Incorporation of ^{13}C-labeled precursors into the xylene ring. J. Biol. Chem. 258, 13431–13437.

[70] Bacher, A., LeVan, Q., Keller, P.J. and Floss, H.G. (1985) Biosynthesis of riboflavin. Incorporation of multiply ^{13}C-labeled precursors into the xylene ring. J. Am. Chem. Soc. 107, 6380–6385.

[71] LeVan, Q., Keller, P.J., Bown, D.H., Floss, H.G. and Bacher, A. (1985) Biosynthesis of riboflavin in *Bacillus subtilis*: Origin of the four-carbon moiety. J. Bacteriol. 162, 1280–1284.

[72] Floss, H.G., LeVan, Q., Keller, P.J. and Bacher, A. (1983) Biosynthesis of riboflavin. An unusual rearrangement in the formation of 6,7-dimethyl-8-ribityllumazine. J. Am. Chem. Soc. 105, 2493–2494.

[73] Volk, R. and Bacher, A. (1991) Biosynthesis of riboflavin. Studies on the mechanism of L-3,4-dihydroxy-2-butanone 4-phosphate synthase. J. Biol. Chem. 266, 20610–20618.

[74] Weber, S., Eisenreich, W., Bacher, A. and Hartmann, T. (1998) Pyrrolizidine alkaloids of the lycopsamine type: Biosynthesis of trachelanthic acid. Phytochemistry (in press).

[75] Fuchs, G. (1989) Alternative pathways of autotrophic CO_2 fixation. In: Autotrophic Bacteria (Schlegel, H.G. and Bowien, B., Eds.), pp. 365–382. Science Tech Publishers, Madison, WI.

[76] Holo, H. and Sirevåg, R. (1986) Autotrophic growth and CO_2 fixation of *Chloroflexus aurantiacus*. Arch. Microbiol. 145, 173–180.

[77] Holo, H. and Grace, D. (1987) Polyglucose synthesis in *Chloroflexus aurantiacus* studied by ^{13}C-NMR. Arch. Microbiol. 148, 292–297.

[78] Holo, H. (1989) *Chloroflexus aurantiacus* secretes 3-hydroxypropionate, a possible intermediate in the assimilation of CO_2 and acetate. Arch. Microbiol. 151, 252–256.

[79] Strauß, G., Eisenreich, W., Bacher, A. and Fuchs, G. (1992) ^{13}C-NMR study of autotrophic CO_2 fixation pathways in the sulfur-reducing archaebacterium *Thermoproteus neutrophilus* and in the phototrophic eubacterium *Chloroflexus aurantiacus*. Eur. J. Biochem. 205, 853–866.

[80] Strauß, G. and Fuchs, G. (1993) Enzymes of a novel autotrophic CO_2 fixation pathway in the phototrophic bacterium *Chloroflexus aurantiacus*, the 3-hydroxypropionate cycle. Eur. J. Biochem. 215, 633–643.

[81] Ishii, M., Miyake, T., Satoh, T., Sagiyama, H., Oshima, Y., Kodama, T. and Igarashi, Y. (1997) Autotrophic carbon dioxide fixation in *Acidianus brierleyi*. Arch. Microbiol. 166, 368–371.

[82] Schäfer, S., Götz, M., Eisenreich, W., Bacher, A. and Fuchs, G. (1989) ^{13}C-NMR study of autotrophic CO_2 fixation in *Thermoproteus neutrophilus*. Eur. J. Biochem. 184, 151–156.

[83] Sauer, U., Hatzimanikatis, V., Bailey, J.E., Hochuli, M., Szyperski, T. and Wüthrich, K. (1997) Metabolic fluxes in riboflavin-producing *Bacillus subtilis*. Nature Biotechnol. 15, 448–452.

[84] Szyperski, T. (1995) Biosynthetically directed fractional ^{13}C-labeling of proteinogenic amino acids. An efficient analytical tool to investigate intermediary metabolism. Eur. J. Biochem. 232, 433–448.

[85] Ugurbil, K., Brown, T.R., DenHollander, J.A., Glynn, P. and Shulman, R.G. (1978) High-resolution ^{13}C nuclear magnetic resonance studies of glucose metabolism in *Escherichia coli*. Proc. Natl. Acad. Sci. USA 75, 3742–3746.

[86] Szyperski, T., Bailey, J.E. and Wüthrich, K. (1996) Detecting and dissecting metabolic fluxes using biosynthetic fractional C-13 labeling and two-dimensional NMR spectroscopy. Trends Biotechnol. 14, 453–459.

[87] Sonntag, K., Schwinde, J., de Graaf, A.A., Marx, A., Eikmanns, B.J., Wiechert, W. and Sahm, H. (1995) C-13 NMR studies of the fluxes in the central metabolism of *Corynebacterium glutamicum* during growth and overproduction of amino acids in batch cultures. Appl. Microbiol. Biotechnol. 44, 489–495.

[88] Schmidt, K., Marx, A., de Graaf, A.A., Wiechert, W., Sahm, H., Nielsen, J. and Villadsen, J. (1998) C-13 tracer experiments and metabolite balancing for metabolic flux analysis: Comparing two approaches. Biotechnol. Bioeng. 58, 254–257.

[89] Marx, A., de Graaf, A.A., Wiechert, W., Eggeling, L. and Sahm, H. (1996) Determination of the fluxes in the central metabolism of *Corynebacterium glutamicum* by nuclear magnetic resonance spectroscopy combined with metabolite balancing. Biotechnol. Bioeng. 49, 111–129.

[90] Shiomi, K., Iinuma, H., Naganawa, H., Isshiki, K., Takeuchi, T. and Umezawa, H. (1987) Biosynthesis of napyradiomycins. J. Antibiot. 40, 1740–1745.

[91] Duvold, T., Bravo, J.M., Pale-Grosdemange, C. and Rohmer, M. (1997) Biosynthesis of 2-C-methyl-D-erythritol, a putative C_5 intermediate in the mevalonate independent pathway for isoprenoid biosynthesis. Tetrahedron Lett. 38, 4769–4772.

[92] Duvold, T., Cali, P., Bravo, J.M. and Rohmer, M. (1997) Incorporation of 2-C-methyl-D-erythritol, a putative isoprenoid precursor in the mevalonate-independent pathway, into ubiquinone and menaquinone of *Escherichia coli*. Tetrahedron Lett. 38, 6181–6184.

[93] Zhou, D. and White, H. (1991) Early steps of isoprenoid biosynthesis in *Escherichia coli*. Biochem. J. 273, 627–634.

[94] Putra, S.R., Lois, L.M., Campos, N., Boronat, A. and Rohmer, M. (1998) Incorporation of [2,3-$^{13}C_2$]- and [2,4-$^{13}C_2$]-D-1-deoxyxylulose into ubiquinone of *Escherichia coli*

via the mevalonate-independent pathway for isoprenoid biosynthesis. Tetrahedron Lett. 39, 23–26.

[95] Britton, G., Goodwin, T.W., Lockley, W.J.S., Mundy, A.P., Patel, N.J. and Englert, G. (1979) Stereochemistry of cyclization in carotenoid biosynthesis: Use of ^{13}C-labelling to elucidate the stereochemical behaviour of the C-1 methyl substituents during zeaxanthin biosynthesis in a flavobacterium. J. Chem. Soc. Chem. Commun. 27–28.

[96] Moldoveanu, M. and Kates, M. (1988) Biosynthetic studies of the polar lipids of *Halobacterium cutirubrum*. Formation of isoprenyl ether intermediates. Biochim. Biophys. Acta 960, 164–182.

[97] Isshiki, K., Tamamura, T., Sawa, T., Naganawa, H., Takeuchi, T. and Umezawa, H. (1987) Biosynthetic studies of terpentecin. J. Antibiot. 40, 1634–1635.

[98] Flesch, G. and Rohmer, M. (1988) Prokaryontic hopanoids: The biosynthesis of the bacteriohopan skeleton. Eur. J. Biochem. 175, 405–411.

[99] Funayama, S., Ishibashi, M., Komiyama, K. and Omura, S. (1990) Biosynthesis of furaquinocins A and B. J. Org. Chem. 55, 1132–1133.

[100] Shin-ya, K., Furihata, K., Hayakawa, Y. and Seto, H. (1990) Biosynthetic studies of naphterpin, a terpenoid metabolite of *Streptomyces*. Tetrahedron Lett. 31, 6025–6026.

[101] Seto, H., Watanabe, H. and Furihata, K. (1996) Simultaneous operation of the mevalonate and non-mevalonate pathways in the biosynthesis of isopentenyl diphosphate in *Streptomyces aeriouvifer*. Tetrahedron Lett. 37, 7979–7982.

[102] Li, S.-M., Hennig, S. and Heide, L. (1998) Biosynthesis of the dimethylallyl moiety of novobiocin via a non-mevalonate pathway. Tetrahedron Lett. 39, 2717–2720.

[103] Cane, D.E., Rossi, T., Tillman, A.M. and Pachlatko, J.P. (1981) Stereochemical studies of isoprenoid biosynthesis. Biosynthesis of pentalenolactone from [U-$^{13}C_6$]glucose and [6-$^{2}H_2$]glucose. J. Am. Chem. Soc. 103, 1838–1843.

[104] Schwender, J., Zeidler, J., Gröner, R., Müller, C., Focke, M., Braun, S., Lichtenthaler, F.W. and Lichtenthaler, H.K. (1997) Incorporation of 1-deoxy-D-xylulose into isoprene and phytol by higher plants and algae. FEBS Lett. 414, 129–134.

[105] Thiel, R., Adam, K.P., Zapp, J. and Becker, H. (1997) Isopentenyl diphosphate biosynthesis in liverworts. Pharm. Pharmacol. Lett. 7, 103–105.

[106] Lichtenthaler, H.K., Schwender, J., Disch, A. and Rohmer, M. (1997) Biosynthesis of isoprenoids in higher plant chloroplasts proceeds via a mevalonate-independent pathway. FEBS Lett. 400, 271–274.

[107] Nabeta, K., Ishikawa, T. and Okuyama, H. (1995) Sesqui- and di-terpene biosynthesis from ^{13}C labelled acetate and mevalonate in cultured cells of *Heteroscyphus planus*. J. Chem. Soc. Perkin Trans. 1, 3111.

[108] Nabeta, K., Kawae, T., Saitoh, T. and Kikuchi, T. (1997) Synthesis of chlorophyll a and β-carotene from ^{2}H and ^{13}C-labelled mevalonates and ^{13}C-labelled glycine in cultured cells of liverworts, *Heteroscyphus planus* and *Lophocolea heterophylla*. J. Chem. Soc. Perkin Trans. 1, 261–267.

[109] Nabeta, K., Saitoh, T., Adachi, K. and Komuro, K. (1998) Biosynthesis of phytyl side-chain of chlorophyll a: apparent reutilization of carbon dioxide evolved during acetate assimilation in biosynthesis of chlorplastidic isoprenoid. J. Chem. Soc. Chem. Commun. 671–672.

[110] Sagner, S., Eisenreich, W., Fellermeier, M., Latzel, C., Bacher, A. and Zenk, M.H. (1998) Biosynthesis of 2-C-methyl-D-erythritol in plants by rearrangement of the terpenoid precursor, 1-deoxy-D-xylulose 5-phosphate. Tetrahedron Lett. 39, 2091–2094.

[111] Sagner, S., Latzel, C., Eisenreich, W., Bacher, A. and Zenk, M.H. (1998) Differential incorporation of 1-deoxy-D-xylulose into monoterpenes and carotenoids in higher plants. J. Chem. Soc. Chem. Commun. 221–222.

[112] Li, S.-M., Hennig, S. and Heide, L. (1998) Shikonin: A geranyl diphosphate-derived plant hemiterpenoid formed via the mevalonate pathway. Tetrahedron Lett. 39, 2721–2724.

[113] Knöss, W., Reuter, B. and Zapp, J. (1997) Biosynthesis of the labdane diterpene marrubiin in *Marrubium vulgare* via a non-mevalonate pathway. Biochem. J. 326, 449–454.

[114] Eisenreich, W., Sagner, S., Zenk, M.H. and Bacher, A. (1997) Monoterpenoid essential oils are not of mevalonoid origin. Tetrahedron Lett. 38, 3889–3892.

[115] Hano, Y., Ayukawa, A., Nomura, T. and Ueda, S. (1994) A chimeric hemiterpene biosynthesis in *Morus alba* cell cultures. Naturwissenschaften 81, 260–262.

[116] Eichinger, D. (1993) Isolierung des Monoterpens Loganin aus *R. serpentina*. Diplomarbeit, Technische Universität, Munich.

[117] Cartayrade, A., Schwarz, M., Jaun, B. and Arigoni, D. (1994) Abstract P1, 2nd Symposium of the European Network on Plant terpenoids, Strasbourg/Bischenberg, 23–27 January 1994.

[118] Schwender, J., Seemann, M., Lichtenthaler, H.K. and Rohmer, M. (1996) Biosynthesis of isoprenoids (carotenoids, sterols, prenyl side-chains of chlorophylls and plastoquinone) via a novel pyruvate/glyceraldehyde-3-phosphate non-mevalonate pathway in the green alga *Scenedesmus obliquus*. Biochem. J. 316, 73–80.

[119] Hasona, A., Ray, R.M. and Shanmugam, K.T. (1998) Physiological and genetic analyses leading to identification of a biochemical role for the *moeA* (molybdate metabolism) gene product in *Escherichia coli*. J. Bacteriol. 180, 1466–1472.

[120] Rajagopalan, K.V. (1996) Biosynthesis of the molybdenum cofactor, in *Escherichia coli* and *Salmonella*: Cellular and Molecular Biology (Neidhardt, F.C., Ed.), 2nd edn., Vol. 1, pp. 674–679. American Society for Microbiology, Washington, DC.